

Josephson-Junction Qubits and the Readout Process by Single-Electron Transistors

Gerd Schön¹, Alexander Shnirman², and Yuriy Makhlin^{1,3}

¹*Institut für Theoretische Festkörperphysik, Universität Karlsruhe, D-76128 Karlsruhe, Germany.*

²*Department of Physics, University of Illinois at Urbana-Champaign, Urbana, IL 61801-3080, U.S.A.*

³*Landau Institute for Theoretical Physics, 117940 Moscow, Russia.*

Several physical realizations of quantum bits have been proposed, including trapped ions, NMR systems and spins in nano-structures, quantum optical systems, and nano-electronic devices. The latter appear most suitable for large-scale integration and potential applications. We suggest to use low-capacitance Josephson junctions, exploiting the coherence of tunneling in the superconducting state combined with the possibility to control individual charges by Coulomb blockade effects. These systems constitute quantum bits (qubits), with logical states differing by one Cooper-pair charge. Single- and two-bit operations can be performed by applying a sequence of gate voltages. The phase coherence time is sufficiently long to allow a series of these steps. The ease and precision of these manipulations depends on the specific design. Here we concentrate on a circuit which is most easily fabricated in an experiment.

In addition to the manipulation of qubits the resulting quantum state has to be read out. This can be accomplished by coupling a single-electron transistor capacitively to the qubit. To describe this quantum measurement process we study the time evolution of the density matrix of the coupled system. Only when a transport voltage is turned on, the transistor destroys the phase coherence of the qubit; in this case within a short time. The measurement is accomplished after a longer time scale, when the signal resolves the different quantum states. At still longer times the measurement process itself destroys the information about the initial state. We present a suitable set of system parameters, which can be realized by present-day technology.

I. INTRODUCTION

The investigation of nano-scale electronic devices, such as low-capacitance tunnel junctions or quantum dot systems, has always been motivated by the perspective of future applications. By now several have been demonstrated, e.g. the use of single-electron transistors (SET) as ultra-sensitive electro-meters and single-electron pumps. From the beginning it also appeared attractive to use these systems for digital operations needed in classical computation (see Ref. 1 for a review). Obviously *single-electron* devices would constitute the ultimate electronic memory. Unfortunately, their extreme sensitivity makes them also very susceptible to fluctuations and random background charges. Due to these problems — and the continuing progress of conventional techniques — the future of SET devices in *classical* digital applications remains uncertain.

The situation is different when we turn to elements for quantum computers. They could perform certain calculations which no classical computer could do in acceptable times by exploiting the quantum mechanical coherent evolution of superpositions of states². Here conventional systems provide no alternative. In this context, ions in a trap, manipulated by laser irradiation is the best studied system^{3,4}. However, alternatives need to be explored, in particular those which are more easily embedded in an electronic circuit. From this point of view nano-electronic devices appear particularly promising.

The simplest choice, normal-metal single-electron devices are ruled out, since — due to the large number of electron states involved — different, sequential tunnel-

ing processes are incoherent. Ultra-small quantum dots with discrete levels, and in particular, spin degrees of freedom embedded in nanostructured materials are candidates. They can be manipulated by tuning potentials and barriers⁵. However, these systems are difficult to fabricate in a controlled way. More attractive appear systems of Josephson contacts, where the coherence of the superconducting state can be exploited and the technology is quite advanced. Macroscopic quantum effects associated with the flux in a SQUID have been demonstrated⁶. Quantum extension of elements based on single flux logic have been suggested⁷, and efforts are made to observe one of the elementary processes, the coherent oscillation of the flux between degenerate states⁸.

We suggest to use low-capacitance Josephson junctions^{9,10}, where Cooper pairs tunnel coherently while Coulomb blockade effects allow the control of individual charges. They provide physical realizations of quantum bits (qubits) with logical states differing by the number of Cooper pair charges on an island. These junctions can be fabricated by present-day technology. The coherent tunneling of Cooper pairs and the related properties of quantum mechanical superpositions of charge states have been discussed and demonstrated in experiments^{11–16}.

We concentrate on the simplest design of the qubit. Although recent modifications¹⁷ to the design permit control over two-bit interactions and offer a possibility of more convenient single-bit manipulations, the simplest circuit allows to introduce the ideas and is easier to fabricate. In Section II we will introduce the system and show how single- and two-bit operations (gates) can be performed by the application of sequences of gate voltages. In Section III we analyze the influence of dissipation and

fluctuations and conclude that for a proper choice of parameters the phase coherence time is sufficiently long to allow a large number of gate operations.

In addition to the controlled manipulations of qubits, quantum computation requires a quantum measurement process to read out the final state. The requirements for both steps appear to contradict each other. During manipulations the dephasing should be minimized, whereas a measurement should dephase the state of the qubit as fast as possible. The option to couple the measuring device to the qubit only when needed is hard to achieve in nano-scale systems. The alternative described in Section IV, is to couple a normal-state single-electron transistor capacitively to a qubit¹⁸. During the manipulations the transport voltage of the SET is turned off, and the SET only acts as an extra capacitor. To perform the measurement the transport voltage is turned on. The dissipative current through the transistor dephases the qubit and provides the read-out signal for the quantum state. We describe this quantum measurement process by considering explicitly the time-evolution of the density matrix of the coupled system. We find that the process is characterized by three time scales: a short dephasing time, the longer ‘measurement time’ when the signal resolves the different quantum states, and finally the mixing time after which the measurement process itself destroys the information about the initial state. Similar nonequilibrium dephasing processes^{19–21} have recently been demonstrated experimentally²².

In Section V we discuss system parameters and suggest suitable sets which can be realized by present-day technology. We further compare with related work.

II. JOSEPHSON JUNCTION QUBITS

A. Qubits and single-bit gates

The simplest Josephson junction qubit is shown in Fig. 1a. It consists of a small superconducting island connected by a tunnel junction, with capacitance C_J and Josephson coupling energy E_J , to a superconducting electrode. An ideal voltage source, V_{qb} , is connected to the

system via a gate capacitor C (fluctuation effects will be discussed later). We choose a material such that the superconducting energy gap Δ is the largest energy in the problem, larger even than the single-electron charging energy to be discussed below. In this case quasi-particle tunneling is suppressed at low temperatures, and a situation can be achieved where no quasiparticle excitations exist on the island*.

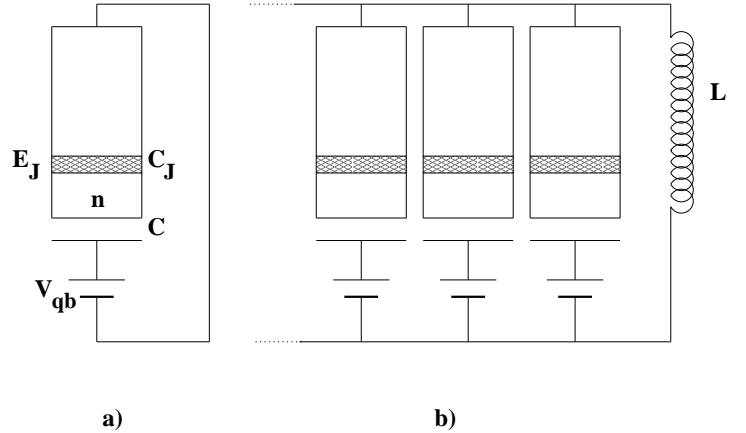


FIG. 1. Idealized a) one qubit and b) multi-qubit systems.

In the following we will consider the situation where only Cooper pairs tunnel in the superconducting junction. This system is described by the Hamiltonian

$$H = 4E_{qb}(n - n_{qb})^2 - E_J \cos \Theta . \quad (1)$$

Here, n is the number (operator) of extra Cooper pair charges on the island (relative to some neutral reference state) and the phase variable Θ is its conjugate $n = \frac{\hbar}{i} \frac{\partial}{\partial(\hbar\Theta)}$. The charging energy of the superconducting island is characterized by the scale $E_{qb} \equiv e^2/2(C + C_J)$, while the dimensionless gate charge, $n_{qb} \equiv CV_{qb}/2e$, acts as a control field. We consider systems where E_{qb} is much larger than the Josephson coupling energy, $E_{qb} \gg E_J$. In this regime a convenient basis is formed by the charge

Under suitable conditions the superconducting state is totally paired, i.e. the number of electrons on the island is even, since an extra quasi-particle (odd number of electrons) costs the extra energy Δ . This ‘parity effect’ has been established in experiments below a crossover temperature $T^ \approx \Delta / \ln N_{eff}$, where N_{eff} is the number of electrons in the system near the Fermi energy^{13,23–25}. For a small enough island, T^* is typically one order of magnitude smaller than the superconducting transition temperature. For the case that — e.g. due to the initial preparation — an unpaired excitation exists on the island, a channel should be provided for the quasiparticle to escape to normal parts of the system²³.

states, parameterized by the number of Cooper pairs n on the island. In this basis the Hamiltonian (1) reads

$$H = \sum_n 4E_{\text{qb}}(n - n_{\text{qb}})^2 |n\rangle\langle n| - \frac{1}{2}E_J(|n\rangle\langle n+1| + |n+1\rangle\langle n|). \quad (2)$$

For most values of n_{qb} the energy levels are dominated by the charging part of the Hamiltonian. However, when n_{qb} is approximately half-integer and the charging energies of two adjacent states are close to each other, the Josephson tunneling mixes them strongly (see Fig. 2).

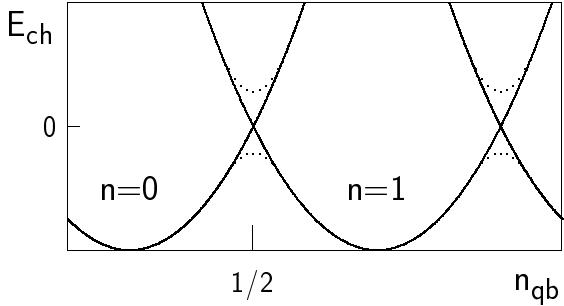


FIG. 2. The charging energy of the superconducting electron box is shown (solid lines) as a function of the gate charge n_{qb} for different numbers of extra Cooper pairs n on the island. Near degeneracy points the weaker Josephson coupling energy mixes the charge states and modifies the energy of the eigenstates (dotted line). In this regime the system effectively reduces to a two-state quantum system.

We concentrate on the voltage interval near a degeneracy point of two charge states, say $n = 0$ and $n = 1$. For the parameters chosen, further charge states can be ignored, and the system (1) reduces to a two-state model, with Hamiltonian which can be written in spin- $\frac{1}{2}$ notation in terms of Pauli spin matrices $\vec{\sigma} = \sigma_x, \sigma_y, \sigma_z$ as

$$H = \frac{1}{2}E_{\text{ch}}(V_{\text{qb}})\sigma_z - \frac{1}{2}E_J\sigma_x. \quad (3)$$

The charge states $n = 0$ and $n = 1$ correspond to the basis states $|\downarrow\rangle \equiv |0\rangle$ and $|\uparrow\rangle \equiv |1\rangle$, respectively. The charging energy $E_{\text{ch}}(V_{\text{qb}}) = 4E_{\text{qb}}(1 - 2n_{\text{qb}})$, equivalent to the field in z -direction, is controlled by the gate voltage. For convenience we can further rewrite the Hamiltonian as

$$H = \frac{1}{2}\Delta E_\eta (\cos \eta \sigma_z - \sin \eta \sigma_x), \quad (4)$$

where the mixing angle $\eta = \tan^{-1}[E_J/E_{\text{ch}}(V_{\text{qb}})]$ determines the direction of the effective magnetic field in the xz -plane, and the energy splitting between the eigenstates is $\Delta E_\eta = \sqrt{E_{\text{ch}}^2(V_{\text{qb}}) + E_J^2} = E_J/\sin \eta$. At the degeneracy point, $\eta = \pi/2$, it reduces to E_J . The eigenstates are denoted in the following as $|0\rangle$ and $|1\rangle$. For some chosen value of n_{qb} they are

$$|0\rangle = \cos \frac{\eta}{2} |\downarrow\rangle + \sin \frac{\eta}{2} |\uparrow\rangle \\ |1\rangle = -\sin \frac{\eta}{2} |\downarrow\rangle + \cos \frac{\eta}{2} |\uparrow\rangle. \quad (5)$$

For later convenience we can rewrite the Hamiltonian in the basis of eigenstates. To avoid confusion we introduce a second set of Pauli matrices, $\vec{\rho}$, which operate in the basis $|0\rangle$ and $|1\rangle$, while reserving $\vec{\sigma}$ for the basis of charge states $|\downarrow\rangle$ and $|\uparrow\rangle$. By definition the Hamiltonian then becomes $H = \frac{1}{2}\Delta E_\eta \rho_z$.

The logical states of the qubit are the eigenstates of the Hamiltonian (4). By changing the gate voltage we can perform the required one-bit operations (gates). If, for example, one chooses the idle state far away from the degeneracy, the logical states $|0\rangle$ and $|1\rangle$ are close to $|\downarrow\rangle$ and $|\uparrow\rangle$, respectively. Then switching the system suddenly to the degeneracy point for a time Δt and then switching back produces a rotation in spin space,

$$U_{\text{1-bit}}(\Delta t) = \exp(i\alpha\sigma_x) = \begin{pmatrix} \cos \alpha & i \sin \alpha \\ i \sin \alpha & \cos \alpha \end{pmatrix}, \quad (6)$$

where $\alpha = E_J\Delta t/2\hbar$. Depending on the value of Δt , a spin flip can be produced, or, starting from $|0\rangle$, a superposition of states with any chosen weights can be reached. Similarly a temporary change of n_{qb} by a small amount changes the energy difference between ground and excited states and hence produces a phase shift, relative to that which would be acquired in the idle state.

The example presented above provides an approximate spin flip for the situation where the idle point is far from degeneracy and $E_{\text{qb}} \gg E_J$. But a spin flip in the logical basis can be performed also in a rigorous way. It requires that we switch from the idle point η_{idle} to the point where the effective magnetic field is orthogonal to the idle one, $\eta = \eta_{\text{idle}} + \pi/2$. This changes the Hamiltonian from $H = \frac{1}{2}\Delta E_{\eta_{\text{idle}}}\rho_z$ to $H = \frac{1}{2}\Delta E_{\eta_{\text{idle}}+\pi/2}\rho_x$. To achieve that, the dimensionless gate charge n_{qb} should be increased by $E_J/(4E_{\text{qb}} \sin 2\eta_{\text{idle}})$. In the limit discussed above, $\eta_{\text{idle}} \ll 1$, the operating point is close to the degeneracy, $\eta = \pi/2$.

Even in the idle state $\eta = \eta_{\text{idle}}$, the energies of the two logical states are different. Hence their phases evolve relative to each other, which leads to the quantum mechanical ‘coherent oscillations’ of a system which is in a superposition of eigenstates. We have to keep track of this time dependence as is demonstrated by the following example (for simplicity again on the approximate level). Imagine we try to perform a rotation by angle α in the spin space, which we can do by a suitable choice of Δt in (6), and after some time delay τ we perform the reverse operation. The unitary transformation for this combined process is

$$\exp(-i\alpha\sigma_x) \cdot \exp\left(i\frac{\Delta E_{\eta_{\text{idle}}}\tau}{2\hbar}\sigma_z\right) \cdot \exp(i\alpha\sigma_x).$$

Clearly the result depends on the intermediate time τ and differs from 1 or a simple phase shift, unless $\Delta E_{\text{idle}}\tau/2\hbar = n\pi$. The time-dependent phase factors, arising from the energy difference in the idle state, can be removed from the logical states if all the calculations are performed in the interaction representation, with zero-order Hamiltonian being the one at the idle point. In this way the information which is contained in the amplitudes of the qubit's states is preserved. However, there is a price for this simplification, namely the transformation to the interaction representation introduces additional time dependence in the Hamiltonian during the operations. Thus a general 1-bit operation induced by switching at t_0 from η_{idle} to η for some time Δt is described by the unitary transformation

$$\mathcal{U}(t_0, \Delta t, \eta) = e^{iH(\eta_{\text{idle}})(t_0+\Delta t)} e^{-iH(\eta)\Delta t} e^{-iH(\eta_{\text{idle}})t_0}. \quad (7)$$

This demonstrates that the effect of the operations depends not only on their time span but also on the moment when they start.

The transformation (7) is the elementary operation in the interaction picture in the sense that it can be performed in one step (one voltage switching). Can we perform an arbitrary single-bit gate using such an operation? To answer this question we note that all the unitary transformations of the two-state system form the group $SU(2)$. The group is three-dimensional, hence one needs in general three controllable parameters to obtain a given single-bit operation. As is obvious from (7), \mathcal{U} depends exactly on three parameters: η , t_0 and Δt . Furthermore, it can be shown that any single-bit gate can be performed in one step if the voltage (i.e. η) and the times t_0 , Δt are chosen properly.[†] (The dependence on t_0 is periodic with the period $\hbar/\Delta E_{\eta_{\text{idle}}}$. Hence the waiting time to a new operation is restricted to this period.)

B. Many-qubit system

For quantum computation a register, consisting of a (large) number of qubits is needed, and pairs of qubits have to be coupled in a controlled way. Such two-bit operations (gates) are necessary, for instance, to create entangled states. For this purpose we couple all qubits by one mutual inductor as shown in Fig. 1b. One can easily

see that for $L = 0$ the system reduces to a series of uncoupled qubits, while for $L = \infty$ they are coupled strongly. Finite values of L introduce some retardation in the interaction. The Hamiltonian of this system, consisting of N qubits and an oscillator formed by the inductance and the total capacitance of all qubits is⁹

$$H = \sum_{i=1}^N \left\{ 4E_{\text{qb}}(n_i - n_{\text{qb},i})^2 - E_J \cos \left(\Theta_i - 2\pi \frac{C_t}{C_J} \frac{\Phi}{\Phi_0} \right) \right\} + \frac{q^2}{2NC_t} + \frac{\Phi^2}{2L}. \quad (8)$$

Here Φ is the flux in the mutual inductor, $\Phi_0 \equiv h/2e$ is the flux quantum, and $q \propto \frac{\partial}{\partial \Phi}$, the variable conjugated to Φ , is related to the total charge on the gate capacitors of the qubits. For the oscillations in this LC -circuit the junction and gate capacitor of each qubit act in series, hence the relevant capacitance is $C_t^{-1} = C_J^{-1} + C^{-1}$. The voltage oscillations of the LC -circuit affect all the qubits equally, thus Φ is coupled to each of the phases Θ_i . The reduction factor C_t/C_J describes the screening of these voltage oscillations by the gate capacitors. We have chosen here to express the coupling via a shift of the phase in the Josephson coupling terms arising from the voltage oscillations. This form is reminiscent of the usual description of SQUIDs, except that here Φ is a dynamics variable and its effect is reduced by the ratio of capacitances. Alternatively, we could have added the oscillating charges to the gate charges in the charging energy. Both forms are equivalent and related by a canonical transformation. This and a more detailed derivation of (8) has been presented in Ref. 9.

The oscillator described by the charge q and flux Φ with characteristic frequency $\omega_{LC}^{(N)} = (NLC_t)^{-1/2}$ produces an effective coupling between the qubits. We choose parameters such that

$$\hbar\omega_{LC}^{(N)} \gg \Delta E_\eta, \quad (9)$$

$$(C_t/C_J)\sqrt{\langle \Phi^2 \rangle} \ll \Phi_0. \quad (10)$$

The first condition (9) assures that the oscillator remains in its ground state at all relevant operation frequencies. I.e. the logical operations on the qubits are not affected by excited states. The second condition (10) prevents the Josephson coupling in (8) from being “washed out” by the fluctuations of Φ . Since they are limited by L , hence

[†]It is customary to consider rotations about two axes, say, x - and z -rotations, as device-independent elementary single-qubit gates. Then, any single-bit gate in a quantum algorithm is described as a combination of three consecutive elementary rotations given by their angles (e.g. Euler angles α , β , γ). To realize such a gate \mathcal{O} we need to solve the equation $\mathcal{U}(\eta, t_0, \Delta t) = \mathcal{O}(\alpha, \beta, \gamma)$ to find the triple of η , t_0 and Δt . Since usually only a few different single-bit gates are used, corresponding triples can be calculated in advance.

$\langle \Phi^2 \rangle / L \approx \frac{1}{2} \hbar \omega_{LC}^{(N)}$, this condition imposes only weak constraints on the parameters.

Although the LC -oscillator remains in its ground state, it provides an effective coupling between the qubits. To analyze this we expand in (8) the Josephson coupling terms in Φ and, because of (10), neglect powers higher than linear. The linear term is $I\Phi$, where the current through the inductor is given by the sum of qubits' contributions,

$$I = \frac{C_t}{C_J} \frac{2\pi E_J}{\Phi_0} \sum_i \sin \Theta_i. \quad (11)$$

The linear term and the unperturbed Hamiltonian of the oscillator can be combined to a square,

$$\frac{q^2}{2NC_t} + \frac{\Phi^2}{2L} + I\Phi = \frac{q^2}{2NC_t} + \frac{(\Phi + LI)^2}{2L} - \frac{LI^2}{2}. \quad (12)$$

As long as the frequency of the oscillator is large compared to characteristic frequencies of the qubit's motion (9), one can use the adiabatic approximation and treat the slow qubit's variables (Θ_i) as constant to find the energy levels of the oscillator. Since the lowest level of the first two terms in the rhs of Eq.(12), equal to $\hbar\omega_{LC}/2$, does not depend on I , the correction to the ground state energy is given by the last term. This term provides the effective coupling between the qubits

$$H_{\text{int}} = -E_L \left(\sum_i \sin \Theta_i \right)^2, \quad (13)$$

where the energy scale is

$$E_L = 2\pi^2 \frac{C_t^2}{C_J^2} \frac{E_J^2 L}{\Phi_0^2}. \quad (14)$$

In the spin- $\frac{1}{2}$ notation $\sin \Theta_i = \frac{1}{2} \sigma_y^{(i)}$ and the interaction term becomes (up to constant terms)

$$H_{\text{int}} = -\frac{E_L}{2} \sum_{i < j} \sigma_y^{(i)} \sigma_y^{(j)}. \quad (15)$$

The ideal system would be one where the coupling between different qubits could be switched on and off, leaving the qubits uncoupled in the idle state and during 1-bit operations. This option requires a more complicated design¹⁷. With the present, simplest model the qubits are coupled at all times. But even in this case we can control the coupling in an approximate way by tuning the

energies of the selected qubits in and out of resonance. If E_L is smaller or comparable to E_J and the gates voltages $V_{qb,i}$ are all different, such that no pairs of qubits is near a degeneracy, the interactions (15) have only weak effects. In this case, the eigenstates of, say, a two-bit system are approximately $|\downarrow\downarrow\rangle$, $|\downarrow\uparrow\rangle$, $|\uparrow\downarrow\rangle$ and $|\uparrow\uparrow\rangle$, which separated by energies are larger than E_L . Hence, the effect of the coupling is weak[†]. If, however, a pair of these state is degenerate, the coupling lifts the degeneracy, changing the eigenstates drastically. For example, if $V_1 = V_2$, the states $|\downarrow\uparrow\rangle$ and $|\uparrow\downarrow\rangle$ are degenerate. In this case the correct eigenstates are: $\frac{1}{\sqrt{2}}(|\downarrow\uparrow\rangle + |\uparrow\downarrow\rangle)$ and $\frac{1}{\sqrt{2}}(|\downarrow\uparrow\rangle - |\uparrow\downarrow\rangle)$ with energy splitting E_L between them.

With the coupling (15) we are able to perform two-bit operations and create, e.g., entangled states. In the idle state we bias all qubits at different voltages. Then we suddenly switch the voltages of two selected qubits to be equal, bringing those two qubits for a time Δt into resonance, and then we switch back. The result is a two-bit operation, which is a rotation in the subspace spanned by $|\downarrow\uparrow\rangle, |\uparrow\downarrow\rangle$:

$$U_{2\text{-bit}}(\Delta t) = \begin{pmatrix} \cos \beta & i \sin \beta \\ i \sin \beta & \cos \beta \end{pmatrix}, \quad (16)$$

where $\beta = E_L \Delta t / 2\hbar$. The states $|\downarrow\downarrow\rangle, |\uparrow\uparrow\rangle$ merely acquire phase factors, relative to what they would acquire in the idle state. For all other qubits the interaction remains a small perturbation.

Similar to the situation with single-bit gates, the many-qubit logical states have time-dependent phase factors and the result of several consecutive 2-bit gates depends on the waiting time between them. Again a transformation to the interaction representation makes this time dependence explicit. To produce any transformation in the subspace $\{|\downarrow\uparrow\rangle, |\uparrow\downarrow\rangle\}$ (3 parameters) combined with any phase shift in the subspace $\{|\downarrow\downarrow\rangle, |\uparrow\uparrow\rangle\}$ (one more parameter), one needs to control four independent parameters. E.g., any such combination can be a result of two consecutive voltage switchings (switching the bias V_1 of the first qubit to the resonance value V_2) with proper chosen starting times and time spans.

The two-bit gates (16) together with all one-bit gates, i.e. spin rotations (6) and the phase shifts, constitute a *universal set*. This means they are sufficient for all manipulations required for quantum computation.

[†]This effect, while weak, still introduces errors and limits the length of the computation. We discuss this effect in Appendix B. We also note that the coupling can be effectively turned off during the idle periods with the use of a sequence of refocusing voltage pulses.

C. Extensions and discussion

To check the experimental feasibility of the present proposal it is necessary to estimate the time-span Δt of the voltage pulses needed for typical single-bit operations. We note that a reasonable value of E_J is of the order of $E_J/k_B = 0.1\text{--}1\text{K}$. It cannot be chosen much smaller, since the condition $k_B T \leq E_J$ should be satisfied, and it should not be much larger since this would increase the technical difficulties associated with the time control. The corresponding time-span is nevertheless short, $\Delta t \approx \hbar/E_J = 10\text{--}100\text{ps}$, and is difficult to control in an experiment.

There exist, however, alternatives. On one hand, a controlled ramping of the coupling energy provides a well defined, though non-trivial single-bit operation. Since in general, any 1-bit gate can be performed with proper choice of 3 controlled parameters, a universal set of gates can be produced in this way. Another possibility is to follow the established procedures of spin resonance experiments. E.g. a coherent spin rotation can be performed as follows: The system is moved adiabatically to the degeneracy point. Then an ac voltage with frequency E_J/\hbar is applied. Finally, the system is moved adiabatically back to the idle point. The time-width of the ac-pulse needed, e.g., for a total spin flip depends on the ac-amplitude, therefore it can be chosen much longer than \hbar/E_J . Unfortunately, in comparison to the sudden switching, the slow adiabatic approach allows only a reduced number of operations during the phase coherence time.

Also the two-bit gates, instead of application of short voltage pulses, can be performed by moving the system adiabatically to a degeneracy point (say $V_1 = V_2$), and then applying an ac voltage pulse in the antisymmetric channel ($V_1 - V_2 \propto \exp(iE_L t)$).

To improve the performance of the device generalizations of the design of the qubits and their coupling may be useful. We mention here one which has been described in Ref. 17. There we discuss a system where the Josephson coupling can be tuned to zero as well. This can be achieved by replacing each Josephson junction by a SQUID with two junctions, and controlling the effective coupling by an applied magnetic flux. While this design is more complicated to realize, it has considerable advantages: (i) In the idle state the Hamiltonian can be tuned to zero ($E_{\text{ch}}(V_{\text{qb}}) = E_{\text{J,eff}} = 0$), which removes the problem that the unitary transformations not only depend on the time span of their duration but also on the time t_0 when they are performed. (ii) The two-bit coupling is turned on only for those two qubits which have both $E_{\text{J,eff}} \neq 0$. (iii) With only $E_{\text{ch}}(V_{\text{qb}})$ or $E_{\text{J,eff}}$ non-zero, the unitary transformations depend in a simple way on the time integral of the corresponding Hamiltonian. Hence ramping the energies produces simple, well-defined gates. As a result of these improvements the manipulations can be performed with much higher accuracy.

III. CIRCUIT EFFECTS: DISSIPATION AND DEPHASING

A. Johnson-Nyquist noise of the gate voltage circuit

The idealized picture outlined above has to be extended to account for the possible dissipation mechanisms causing decoherence and energy relaxation. We focus on the dissipation and fluctuations which originate from the circuit of the voltage sources. In Fig. 3 the equivalent circuit of a qubit coupled to an impedance $Z(\omega)$ is shown. The latter is responsible for current fluctuations with power spectrum

$$\langle \delta I \delta I \rangle_\omega \equiv \int_{-\infty}^{\infty} dt e^{i\omega t} \frac{1}{2} \langle \delta I(t) \delta I(0) \rangle = \text{Re}\{Z^{-1}(\omega)\} \hbar \omega \coth\left(\frac{\hbar\omega}{k_B T}\right). \quad (17)$$

They produce voltage fluctuations at the site of the qubit, to be added to the applied gate voltage, with spectrum

$$\langle \delta V \delta V \rangle_\omega = \text{Re}\{Z_t(\omega)\} \hbar \omega \coth\left(\frac{\hbar\omega}{k_B T}\right), \quad (18)$$

where $Z_t(\omega) = [i\omega C_t + Z^{-1}(\omega)]^{-1}$.

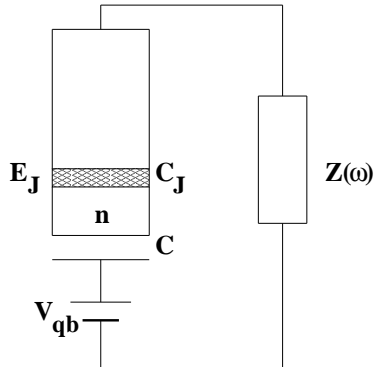


FIG. 3. Qubit with electromagnetic environment.

This linear dissipative element can be modeled by an infinite bath of harmonic oscillators with suitable chosen frequencies and coupling strengths²⁶. The full Hamiltonian of this system thus reads

$$H = 4E_{\text{qb}} \left(n - n_{\text{qb}} - \frac{C \delta V}{2e} \right)^2 - E_J \cos \Theta + H_{\text{bath}}, \quad (19)$$

where $\delta V = \sum_\alpha \lambda_\alpha x_\alpha$, and

$$H_{\text{bath}} = \sum_\alpha \left[\frac{p_\alpha^2}{2m_\alpha} + \frac{m_\alpha \omega_\alpha^2}{2} x_\alpha^2 \right]. \quad (20)$$

When evaluating the correlation functions of $\delta V(t)$ in terms of harmonic oscillator properties, we note that the parameters of the model appear in the combination $J(\omega) \equiv \frac{\pi}{2} \sum_{\alpha} \frac{\lambda_{\alpha}^2}{m_{\alpha}\omega_{\alpha}} \delta(\omega - \omega_{\alpha})$. If we choose this function as $J(\omega) = \omega \text{Re}\{Z_t(\omega)\}$, the oscillator bath produces the voltage fluctuations (18). To be specific we will concentrate in the following on the fluctuations due to an Ohmic resistor R in the bias voltage circuit.

B. Relaxation and dephasing rates

In general, the environment has two effects: inelastic energy relaxation and dephasing, both characterized by their respective time scales, Γ_{in}^{-1} and Γ_{ϕ}^{-1} . To illustrate this point we consider a qubit prepared in a superposition of eigenstates (logical states) $a|0\rangle + b|1\rangle$ with non-vanishing coefficients a and b . This corresponds to an initial density matrix $\hat{\sigma} = \begin{pmatrix} |a|^2 & a^*b \\ ab^* & |b|^2 \end{pmatrix}$. In this case, one question is how fast the diagonal elements of the density matrix relax to their thermal equilibrium values. This relaxation is determined by Γ_{in} . The second question is how fast the off-diagonal elements vanish, which is governed by the rate Γ_{ϕ} . In general, the two rates are not equal.

Influence of the electromagnetic environment on the energy relaxation was discussed in Refs. 27–30 within the Golden rule approach. Both inelastic transitions and dephasing were addressed earlier in the context of spin-boson models, in particular for a two-level system with purely Ohmic dissipation^{31,32}. Our system (19) reduces to a spin-boson model in the limit where only two charge states need to be considered, with a harmonic oscillator bath coupling to σ_z . It still differs from an Ohmic model due to the frequency dependence in the function $Z_t(\omega)$. However, for the relevant frequencies we have $\omega \ll 1/RC_t$, and the physics is dominated by the resistor. Hence we can take over the results from the model calculations of Refs. 31,32 for purely Ohmic environments.

The strength of the fluctuations and, hence, the relaxation and dephasing effects are controlled by the resistance of the circuit. It turns out that it has to be measured in units of the quantum resistance $R_K \equiv h/e^2 \approx 25.8\text{k}\Omega$. Hence for low circuit resistances in the range of $R \approx 50\Omega$ we can hope for a weak effect. Furthermore, in our system the effect of fluctuation is reduced due to the weak capacitive coupling of the qubit to the circuit. Indeed, as is apparent from (19) the coupling of $\delta V(t)$ to the qubit's charge n involves the ratio $C/(C_J + C) = C_t/C_J \ll 1$. Thus, the relevant parameter characterizing the effect of the voltage fluctuations is $(R/R_K)(C_t/C_J)^2$.

In Ref. 31 only the unbiased case of the spin-boson model, corresponding to the qubit at the degeneracy point $n_{\text{qb}} = 1/2$, has been analyzed rigorously. It was found that in this case the two rates are related by

$$\Gamma_{\phi} = \frac{1}{2}\Gamma_{\text{in}} = 2\pi \frac{R}{R_K} \left(\frac{C_t}{C_J} \right)^2 \frac{E_J}{\hbar} \coth \frac{E_J}{2k_B T} . \quad (21)$$

The biased case of the spin-boson model (i.e. the qubit out of the degeneracy) was treated in Ref. 32. In this case, the two rates, expressed in terms of the mixing angle introduced in (5), are

$$\Gamma_{\text{in}} = \sin^2 \eta 4\pi \frac{R}{R_K} \left(\frac{C_t}{C_J} \right)^2 \frac{\Delta E}{\hbar} \coth \frac{\Delta E}{2k_B T} , \quad (22)$$

and

$$\Gamma_{\phi} = \frac{1}{2}\Gamma_{\text{in}} + \cos^2 \eta 8\pi \frac{R}{R_K} \left(\frac{C_t}{C_J} \right)^2 \frac{k_B T}{\hbar} . \quad (23)$$

We note that out of the degeneracy the dephasing rate acquires a component proportional to the temperature.

In addition to the relaxation of diagonal and off-diagonal elements in the basis of the eigenstates (logical states), which are described by the rates given above, the off-diagonal elements carry an oscillating phase factor. The last is related to the ‘coherent oscillations’, which are observed in the evolution of the states in the charge basis or, equivalently, in the quantity $\langle \sigma_z(t) \rangle$. In the absence of dissipation this quantity oscillates coherently around some average value. With dissipation, the average value relaxes to equilibrium with rate Γ_{in} , while the oscillations decay with rate Γ_{ϕ} .

The factors $\sin^2 \eta$ and $\cos^2 \eta$ in Eqs. (22,23) indicate the nature of different contributions to the relaxation and dephasing rates. In the logical basis (5) the qubit's part of the Hamiltonian (19) is diagonal. However, the circuit electromagnetic fluctuations couple to the charge. Hence, in the notation introduced after (5) we have

$$H_{\text{em}} = -\frac{C_t}{C_J} 2e \delta V \sigma_z = -\frac{C_t}{C_J} 2e \delta V (\cos \eta \rho_z + \sin \eta \rho_x) . \quad (24)$$

Since the first term commutes with the qubit's Hamiltonian, only the second one in (24) contributes to the transitions between the logical states. This explains the factor $\sin^2 \eta$ in (22). The first term in (24), while ineffective for transitions, makes the energy difference between the qubit's levels fluctuate. Therefore, the off-diagonal elements of the density matrix acquire a random phase. The last process is “pure” dephasing. It occurs even when transitions are suppressed (e.g. when $E_J = 0$).

We conclude that the dephasing of the initial quantum state of the qubit is caused by two different processes: the dissipative transitions between the logical levels, and the fluctuations of the energy difference between the levels. The off-diagonal elements of the density matrix are suppressed by both of them. While the first process survives at low temperature, the second one produces the dephasing rate proportional to the temperature. Note, however, that at the degeneracy point $\cos \eta = 0$, i. e. there are no

fluctuations of the energy levels, and both dephasing and energy relaxation are due to the transitions.

These results should be taken into account when selecting the optimum idle state for the qubit. If the temperature is low, $k_B T \ll E_J$, the best choice is obviously far from the degeneracy point ($\sin \eta \ll 1$). Also at higher temperatures this regime has a longer coherence time than the degeneracy point, although only by a numerical factor. In all cases it is pure dephasing, rather than inelastic transitions which sets the upper coherence limit at the idle point.

C. Discussion and extensions

In summary, the dephasing rate is small if the effective resistance of the circuit is low compared to the quantum resistance, R_K . Furthermore, a low gate capacitance C reduces the coupling of the qubit to the environment. Hence, with suitable parameters ($R \leq 50\Omega$, $C/C_J \leq 0.1$) at low temperatures the number of operations which can be performed before the environment destroys the phase coherence may be as large as 10^3 – 10^4 . The value of the phase coherence time in this case is of the order of 10–100 ns. Coherence times of this order of magnitude have been observed in experiments on quantum dots³³.

Longer phase coherence times would be achieved if the coupling of the qubit to the noisy environment could be further reduced, without weakening the coupling to the common inductor L which provides the 2-bit coupling. The model discussed above is not ideal since the Ohmic resistor with Johnson-Nyquist noise is assumed to be in the immediate vicinity of the qubit, reduced in its effect only by a low gate capacitor. A suitable design with a combination of superconducting leads and filters can drastically improve the situation.

If the physical dephasing effects are reduced, the more serious will be the errors related to imperfections in the time control or imprecise parameters and coupling energies. In Appendix B we estimate the error introduced by a non-vanishing 2-bit coupling during the idle periods which limits the number of coherent operations. This analysis can be extended to other similar sources. If the combination of all these effects is sufficiently reduced, allowing for 10^4 – 10^5 coherent manipulations steps, then eventually the remaining errors can be corrected by suitable codes³⁴. It is clear from our analysis that this goal can be reached with Josephson junction qubits.

IV. MEASURING THE STATE OF THE QUBIT

A. The model for a single-electron transistor attached to the qubit

The read-out of the state of the qubit requires a quantum measurement process. Since the relevant quantum

degree of freedom is the charge of the qubit island, the natural choice of measurement device is a single-electron transistor (SET). This system is shown in Fig. 4. The left part is the qubit, with state characterized by the number of extra Cooper pairs, n , on the island, and controlled by its gate voltage, V_{qb} . The right part shows a normal island between two normal leads, which form the SET. Its charging state is characterized by the number of extra single-electron charges on the middle island, N . It is controlled by gate and transport voltages, V_g and V_{tr} , and further, due to the capacitive coupling to the qubit, by the state of the latter. A similar setup has recently been studied in the experiments of Refs. 11 with the purpose to demonstrate that the ground state of a single Cooper pair box is a coherent superposition of different charge states. We will discuss the relation of these experiments to our proposal below.

During the quantum manipulations of the qubit the transport voltage V_{tr} across the SET transistor is kept zero and the gate voltage of the SET is chosen to tune the island away from degeneracy points. Therefore no dissipative currents flow in the system, and the transistor merely modifies the capacitances of the system. To perform a measurement one tunes the SET by V_g to the vicinity of its degeneracy point and applies a small transport voltage V_{tr} . The resulting normal current through the transistor depends on the charge configuration of the qubit, since different charge states induce different voltages on the middle island of the SET transistor. In order to investigate whether the dissipative current through the SET transistor allows us to resolve different quantum states of the qubit, we have to discuss various noise factors, including the shot noise associated with the tunneling current and the measurement induced transitions between the states of the qubit. For this purpose we analyze the time evolution of the density matrix of the composite system. We find that for suitable parameters, which can be realized experimentally, the dephasing by the passive SET is weak. When the transport voltage is turned on the dephasing is fast, and the current through the transistor — after a transient period — provides a measure of the state of the qubit. At still longer times the dynamics of the SET destroys the information of the quantum state to be measured.

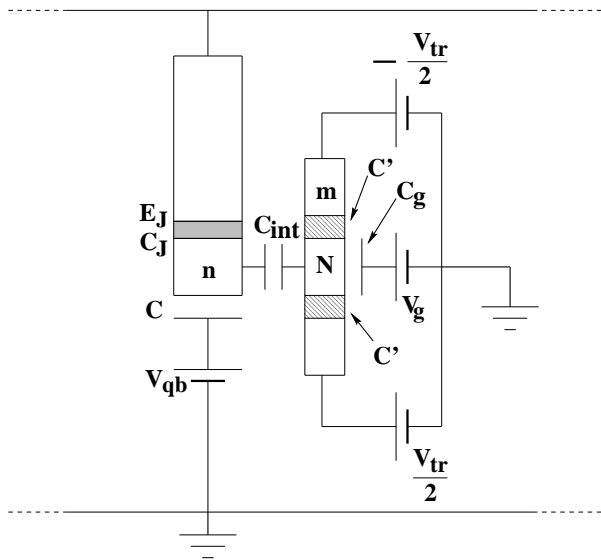


FIG. 4. The circuit consisting of a qubit plus a SET transistor used as a measuring device.

The Hamiltonian of the composite system consists of three main parts

$$H = H_{\text{ch}} + H_L + H_R + H_I + H_J + H_T \quad (25)$$

the charging energy, the terms describing the microscopic degrees of freedom of the metal islands and electrodes, and the tunneling terms, including the Josephson coupling. The charging term is a quadratic form in the variables n and N , for the system shown in Fig. 4 it is

$$H_{\text{ch}}(n, N, V_n, V_N) = 4E_{\text{qb}}n^2 + E_{\text{set}}N^2 + 2E_{\text{int}}nN + 2enV_n + eNV_N. \quad (26)$$

The charging energy scales E_{qb} , E_{set} and E_{int} are determined by the capacitances between all the islands. Introducing

$$A \equiv (C + C_J)(C_g + C_{\text{int}} + 2C') + C_{\text{int}}(C_g + 2C') \approx 2C_JC',$$

we can write them as

$$\begin{aligned} E_{\text{qb}} &= e^2(C_g + C_{\text{int}} + 2C')/2A \approx e^2/2C_J, \\ E_{\text{set}} &= e^2(C + C_{\text{int}} + C_J)/2A \approx e^2/(4C'), \\ E_{\text{int}} &= e^2C_{\text{int}}/A \approx e^2C_{\text{int}}/(2C_JC'). \end{aligned} \quad (27)$$

Here we have assumed that the two junctions of the SET have equal capacitances C' , and the approximate results refer to the limit $C, C_{\text{int}}, C_g \ll C' \ll C_J$, which we consider useful (see below). The effective gate voltages V_n and V_N depend in general on all voltages V_{qb} , V_g , and the voltages applied to both electrodes of the SET. However, for a symmetric setup (equal junction capacitances) and symmetric distribution of the transport voltage, V_{tr} , between both electrodes of the SET (as shown in Fig. 4), V_n and V_N are controlled only by the two gate voltages,

$$\begin{aligned} V_N &= V_g \frac{C_g(C + C_{\text{int}} + C_J)}{A} + V_{\text{qb}} \frac{C_{\text{int}}C}{A}, \\ V_n &= V_g \frac{C_gC_{\text{int}}}{A} + V_{\text{qb}} \frac{(C_g + C_{\text{int}} + 2C')C}{A}. \end{aligned} \quad (28)$$

The microscopic terms describe noninteracting electrons in the two leads and on the middle island of the SET transistor

$$H_r = \sum_{k\sigma} \epsilon_{k\sigma}^r c_{k\sigma}^{r\dagger} c_{k\sigma}^r \quad (r = \text{L, R, I}). \quad (29)$$

The index σ labels transverse channels including the spin, while k labels the wave vector within one channel.

Similar terms describe the electrode and island of the qubit; however, for the superconducting non-dissipative element the microscopic degrees of freedom can be integrated out³⁵, resulting in the “macroscopic” quantum description presented in Sect. II. In this procedure the tunneling terms reduce to the Josephson coupling $H_J = -E_J \cos \Theta$, expressed in a collective variable describing the coherent transfer of Cooper pairs in the qubit, $e^{i\Theta}|n\rangle = |n+1\rangle$.

The normal electron tunneling in the SET transistor is described by the standard tunneling Hamiltonian, which couples the microscopic degrees of freedom,

$$H_T = \sum_{kk'\sigma} T_{kk'\sigma}^L c_{k\sigma}^{L\dagger} c_{k'\sigma}^L e^{-i\phi} + \sum_{k'k''\sigma} T_{k'k''\sigma}^R c_{k''\sigma}^{R\dagger} c_{k'\sigma}^R e^{-i\phi} e^{i\psi} + \text{h.c.} \quad (30)$$

To make the charge transfer explicit, (30) displays two “macroscopic” operators, $e^{\pm i\phi}$ and $e^{\pm i\psi}$. The first one describes changes of the charge on the transistor island due to the tunneling: $e^{i\phi}|N\rangle = |N+1\rangle$. It may be treated as an independent degree of freedom if the total number of electrons on the island is large. We further include the operator $e^{\pm i\psi}$ which describes the changes of the charge in the right lead. It acts on m , the number of electrons which have tunneled through the SET transistor, $e^{i\psi}|m\rangle = |m+1\rangle$. Since the chemical potential of the right lead is controlled, m does not appear in any charging part of the Hamiltonian. However, we have to keep track of it, since it is the measured quantity, related to the current through the SET transistor.

In equilibrium, i.e. when the SET is kept in the state $N = 0$, the qubit’s dynamics is described by the same Hamiltonian as discussed in previous sections, $H_{\text{qb}} = 4E_{\text{qb}}(n - n_{\text{qb}})^2 - E_J \cos \Theta$, where $n_{\text{qb}} \equiv -eV_n/4E_{\text{qb}}$. We recall that in the limit where only the lowest energy charge states $n = 0$ and $n = 1$ are relevant, it reduces to a two state quantum system. In the basis of eigenstates (5), $|0\rangle$ and $|1\rangle$, which are expressed in terms of the mixing angle η , where $\tan \eta = E_J/E_{\text{ch}}(n_{\text{qb}})$, it becomes $H_{\text{qb}} = \frac{1}{2}\Delta E_\eta \rho_z$, where $\Delta E_\eta \equiv E_J/\sin \eta$. In this basis the number operator n becomes non-diagonal,

$$n = \frac{1}{2}(1 + \sigma_z) = \frac{1}{2}(1 + \cos \eta \rho_z + \sin \eta \rho_x) . \quad (31)$$

For the following discussion we choose n_{qb} away from the degeneracy point, which combined with $E_J \ll E_{\text{qb}}$ implies $\tan \eta \ll 1$.

The mixed term in (26) provides the interaction Hamiltonian. With n given by (31) it becomes

$$H_{\text{int}} = E_{\text{int}} N (\cos \eta \rho_z + \sin \eta \rho_x) , \quad (32)$$

plus an extra term, $E_{\text{int}} N$, which together with further terms is collected in the Hamiltonian of the SET transistor,

$$H_{\text{set}} = E_{\text{set}} (N - N_{\text{set}})^2 + H_{\text{L}} + H_{\text{R}} + H_{\text{I}} + H_{\text{T}} . \quad (33)$$

The transistor's gate charge became $N_{\text{set}} \equiv -(eV_N + E_{\text{int}})/2E_{\text{set}}$. The total Hamiltonian thus reads $H = H_{\text{qb}} + H_{\text{set}} + H_{\text{int}}$.

The total system composed of qubit and SET is described by a total density matrix $\hat{\rho}(t)$, which we can reduce, by taking a trace over the microscopic states of the left and right leads and of the island, to $\hat{\sigma}(t) = \text{Tr}_{\text{L,R,I}}\{\hat{\rho}(t)\}$. In general, this reduced density matrix $\hat{\sigma}(i, i'; N, N'; m, m')$ is still a matrix in the index i , which stand for the quantum states of the qubit $|0\rangle$ or $|1\rangle$, in N , and in m . In the following we will assume that initially — as a result of previous quantum manipulations — the qubit is prepared in the quantum state $a|0\rangle + b|1\rangle$, and at time $t = 0$ we switch on a transport voltage to the single-electron transistor. We then can proceed in two different ways, further reducing the density matrix which provides complementary descriptions of the measuring process.

The first, widely used procedure²¹ is to trace over N and m . This yields a reduced density matrix of the qubit $\sigma_{i,j} \equiv \sum_{N,m} \hat{\sigma}(i, j; N, N; m, m)$. Just before the measurement, it is in the state

$$\hat{\sigma}(0) = \begin{pmatrix} |a|^2 & ab^* \\ a^*b & |b|^2 \end{pmatrix} . \quad (34)$$

The questions then arise how fast the off-diagonal elements of $\hat{\sigma}_{i,j}$ vanish, i.e. how fast is the dephasing, and how fast the diagonal elements change their values after the SET is switched to the dissipative state. These questions are the same as in our discussion of fluctuation effects in Section III. However, the coupling to the dissipative SET will shorten these times. This description is enough when one is interested in the quantum properties of the measured system i.e. the qubit only, and the measuring device serves merely as a source of dephasing^{19–22}. It does not tell us much about the quantity measured in an experiment, namely the current flowing through the SET.

The second procedure, pursued in the following, is to evaluate the probability distribution of the number of electrons m which tunnel through the SET during time t ,

$$P(m, t) \equiv \sum_{N,i} \hat{\sigma}(i, i; N, N; m, m)(t) . \quad (35)$$

This distribution provides the information about the experimentally accessible quantity during the measurement process. At $t = 0$ no electrons have tunneled, so $P(m, 0) = \delta_{m,0}$. Then this peak moves in positive m -direction and, simultaneously, it widens due to shot noise. Since two states of the qubit correspond to different tunneling currents, and hence shift velocities in m -direction, one may hope that after some time the peak splits into two. If after sufficient separation of the two peaks their weights are still close to $|a|^2$ and $|b|^2$, a good quantum measurement has been performed. After a longer time further processes destroy this idealized picture. The two peaks transform into a broad plateau, since transitions between the qubit's states are induced by the measurement. Therefore, one should find an optimum time for the measurement, such that, on one hand, the two peaks are separate and, on the other hand, the induced transitions have not yet influenced the process. In order to describe this we have to analyze the time evolution of the reduced density matrix quantitatively.

B. Quantitative description of the measurement process

The time evolution of the density matrix leads to Bloch-type master equations with coherent terms. Examples have recently been analyzed in contexts similar to the present^{36,37,21}. In Ref. 36 a diagrammatic technique has been developed which provides a formally exact master equation as an expansion in the tunneling term H_{T} , while all other terms constitute the zeroth order Hamiltonian $H_0 \equiv H - H_{\text{T}}$, which is treated exactly. The time evolution of the reduced density matrix is given by $\hat{\sigma}(t) = \int dt' \Pi(t, t') \hat{\sigma}(t')$. The propagator $\Pi(t, t')$ can be expressed in a diagrammatic form and finally summed up in a way reminiscent of a Dyson equation. Examples are shown in Fig. 5. In contrasts to ordinary many-body expansions, since the time dependence of the density matrix is described by a forward and a backward time-evolution operator, there are two propagators, which are represented by two horizontal lines (Keldysh contour). The two bare lines describe the coherent time evolution of the system. They are coupled due to the tunneling in the SET, which is treated as a perturbation. The sum of all distinct transitions defines a ‘self-energy’ diagram Σ . Below we will present the rules how to calculate Σ and present a suitable approximate form. The Dyson equation is equivalent to a (generalized) master equation for the density matrix, which reads

$$\frac{d\hat{\sigma}(t)}{dt} - \frac{i}{\hbar} [\hat{\sigma}(t), H_0] = \int_0^t dt' \hat{\sigma}(t') \Sigma(t - t') . \quad (36)$$

In the present problem the density matrix is a matrix $\hat{\sigma}(i, i'; N, N'; m, m') \equiv \hat{\sigma}_{i,N,m}^{i',N',m'}$ in all three indices i ,

N , and m , and the (generalized) transition rates due to single-electron tunneling processes (in general of arbitrary order), $\Sigma_{i,N,m \rightarrow \bar{i},\bar{N},\bar{m}}(t - t')$, connect these diagonal and off-diagonal states.

$$\Pi = \Pi^{(0)} + \Pi^{(0)} \Sigma \Pi^{(0)}$$

FIG. 5. The Dyson-type equation governing the time evolution of the density matrix. It is equivalent to the generalized master equation (36). The ‘self energy’ diagrams Σ describes the transitions due to tunneling in the SET transistor.

The transition rates can be calculated diagrammatically in the framework of the real-time Keldysh contour technique. We briefly review the rules for their evaluation; for more details including the discussion of higher order diagrams we refer to Ref. 36. Typical diagrams, which will be analyzed below, are displayed in Fig. 6 and 7. Again the horizontal lines describe the time evolution of the system governed by the zeroth order Hamiltonian H_0 . Their properties will be discussed below. The directed dashed lines stand for tunneling processes, in the example considered the tunneling takes place in the left junction. According to the rules³⁶ the dashed lines contribute the following factor to the self-energy Σ ,

$$- \alpha_L \left(\frac{\pi}{\hbar \beta} \right)^2 \frac{e^{\pm i \mu_L (t - t')}}{\sinh^2 \left[\frac{\pi}{\hbar \beta} (t - t' \pm i \delta) \right]}, \quad (37)$$

where $\alpha_L \equiv \hbar/(4\pi^2 e^2 R_{T,L})$ is the dimensionless tunneling conductance, μ_L the electro-chemical potential of the left lead, and $\delta \equiv 1/\omega_c$ the inverse frequency cut-off. The sign of the infinitesimal term $i\delta$ depends on the time-direction of the dashed line. It is negative if the direction of the line with respect to the Keldysh contour coincides with its direction with respect to the absolute time (from left to right), and positive otherwise. For example the right part of Fig. 6 should carry a minus sign, while the left part carries a plus sign. Furthermore, the sign in front of $i\mu_L(t - t')$ is negative (positive), if the line goes forward (backward) with respect to the absolute time.

$$\sum_{N,m,i \rightarrow N+1,m,i}^{N,m,j \rightarrow N+1,m,j} = t' + t$$

FIG. 6. Example of a ‘self energy’ diagram for an “in” rate.

$$\sum_{N,m,i \rightarrow N,m,i}^{N,m,j \rightarrow N,m,j} = t' + t$$

FIG. 7. Example of a ‘self energy’ diagram for an “out” rate.

The horizontal lines describe the time-evolution of the system between tunneling processes. For an isolated transistor island they reduce to simple exponential factors $e^{\pm i E(t - t')}$, depending on the charging energy of the system. In the present case, however, where the island is coupled to the qubit we have to account for the nontrivial time evolution of the latter. For instance, the upper line in the left part of Fig. 6 corresponds to $\langle N, j | e^{-i H_0(t - t')} | N, j' \rangle$, while the lower line corresponds to $\langle N+1, i | e^{i H_0(t - t')} | N+1, i' \rangle$. The qubit states $|i\rangle$, $|j\rangle$ in these propagators are the bare ones describing the qubit when the SET is switched off, $N = 0$. As a result, when the SET is in a state with $N \neq 0$, the propagators do not reduce to simple phase factors. To evaluate them we diagonalize H_0 for each value of N . The eigen-energies are given by the SET energy $E_{\text{set}}^N \equiv E_{\text{set}}(N - N_{\text{set}})^2$ plus the eigen-energies of the interacting qubit, $H_{\text{qb}} + H_{\text{int}}$. These are

$$E_{0/1}^N = \mp \frac{1}{2} \Delta E_{\eta}^N, \quad (38)$$

$$\Delta E_{\eta}^N = [(\Delta E_{\eta} + 2E_{\text{int}}N \cos \eta)^2 + (2E_{\text{int}}N \sin \eta)^2]^{1/2}.$$

These energies refer to the exact eigenstates of the interacting qubit, which evolve from the bare qubit states $|0\rangle$ and $|1\rangle$. This correspondence is unambiguous when N is not too large. The exact eigenstates are linear combinations of the bare qubit states with coefficients expressed by mixing angles ϵ_N (analogous to η) given by $\tan \epsilon_N = 2E_{\text{int}}N \sin \eta / (\Delta E_{\eta} + 2E_{\text{int}}N \cos \eta)$. Taking this into account we find the results for the propagators:

$$\begin{aligned} & \langle N, 0 | e^{-i H_0 \Delta t} | N, 0 \rangle \\ &= (\cos^2 \frac{\epsilon_N}{2} e^{-i E_0^N \Delta t} + \sin^2 \frac{\epsilon_N}{2} e^{-i E_1^N \Delta t}) e^{-i E_{\text{set}}^N \Delta t}, \\ & \langle N, 1 | e^{-i H_0 \Delta t} | N, 1 \rangle \\ &= (\cos^2 \frac{\epsilon_N}{2} e^{-i E_1^N \Delta t} + \sin^2 \frac{\epsilon_N}{2} e^{-i E_0^N \Delta t}) e^{-i E_{\text{set}}^N \Delta t}, \\ & \langle N, 1 | e^{-i H_0 \Delta t} | N, 0 \rangle \\ &= \frac{1}{2} \sin \epsilon_N (e^{-i E_0^N \Delta t} - e^{-i E_1^N \Delta t}) e^{-i E_{\text{set}}^N \Delta t}. \end{aligned} \quad (39)$$

During the measurement the transitions between the logical states of the qubit (mixing) should be minimized. To assure this we bias the qubit away from its degeneracy point, and choose $\Delta E \gg E_{\text{int}}, E_J$. In this case, for all relevant values of N , the mixing angles are small, $\epsilon_N \propto N E_{\text{int}} E_J / (\Delta E)^2$. Hence, for the calculation of Σ we keep only terms linear in ϵ_N in (39). This means that for the tunneling processes where the state of the qubit

does not change (first two propagators in (39)) we neglect the $\sin^2(\epsilon_N/2)$ terms and put $\cos^2(\epsilon_N/2)$ equal to 1. We keep, however, the contribution of the third propagator in (39), which is the dominant signature of the time evolution and mixing of the qubit states. The linearization in ϵ_N reduces the number of diagrams we have to evaluate. It is, however, straightforward to extend the calculation to the general case.

In principle the density matrix is an arbitrary non-diagonal matrix in all three indices i , N , and m . But, as has been shown in Ref. 36, a closed set of equations can be derived, describing the time evolution of the system, which involves only the diagonal elements in N . The same is true for the matrix structure in m . Therefore, we need to consider only the following elements of the density matrix $\hat{\sigma}_{j,N,m}^{i,N,m}$. Accordingly, of all the transition rates we need to calculate only those between the corresponding elements of the density matrix, i.e. $\Sigma_{j',N',m' \rightarrow j,N,m}^{i',N',m'}(\Delta t)$. In the present problem we further can assume that the tunneling conductance of the SET is low compared to the inverse quantum resistance. In this case, lowest order perturbation theory in the single electron tunneling, describing ‘sequential tunneling processes’, is sufficient. The diagrams for Σ can be split into two classes, depending on whether they provide expressions for off-diagonal ($N' \neq N$) or diagonal ($N' = N$) in N elements of Σ . In analogy to the scattering integrals in the Boltzmann equation these can be labeled ‘in’ and ‘out’ terms, in the sense that they describe the increase or decrease of a given element $\hat{\sigma}_{j,N,m}^{i,N,m}$ of the density matrix due to transitions from or to other N -states. Examples for the ‘in’ and ‘out’ terms are shown in Fig. 6 and Fig. 7, respectively.

We now are ready to evaluate the rates in Fig. 6 and Fig. 7 in leading order in ϵ_N . As an example we consider an ‘in’ tunneling process in the left junction with the qubit remaining in the diagonal state $|0\rangle$, $(i' = j' = 0, N, m) \rightarrow (i = j = 0, N + 1, m)$. The result is

$$\Sigma_{0,N,m \rightarrow 0,N+1,m}^{0,N,m \rightarrow 0,N+1,m}(\Delta t) = \frac{-\alpha_L(\frac{\pi}{\hbar\beta})^2 e^{-i\tilde{E}_{L,0}\Delta t}}{\sinh^2\left[\frac{\pi}{\hbar\beta}(\Delta t + i\delta)\right]} + \text{c.c.}, \quad (40)$$

where $\tilde{E}_{L,0}$ stands for the change in charging energy in the process

$$\tilde{E}_{L,0} = \mu_L + (E_{\text{set}}^N - E_{\text{set}}^{N+1}) + (E_0^N - E_0^{N+1}). \quad (41)$$

With sufficient accuracy (the derivation is given in Appendix A) this rate (40) reduces to the Golden-rule expression, which at low temperatures, $k_B T \ll \tilde{E}$, becomes

$$\Sigma_{0,N,m \rightarrow 0,N+1,m}^{0,N,m \rightarrow 0,N+1,m}(\Delta t) \approx \Gamma_{L,0} \delta(\Delta t),$$

$$\Gamma_{L,0} = 2\pi\alpha_L \tilde{E}_{L,0} \Theta(\tilde{E}_{L,0}). \quad (42)$$

Analogously, there exists a dual ‘out’ process with rate

$$\Sigma_{0,N,m \rightarrow 0,N,m}^{0,N,m \rightarrow 0,N,m}(\Delta t) \approx -\Gamma_{L,0} \delta(\Delta t). \quad (43)$$

The expression (42) corresponds to the so-called orthodox theory of single-electron tunneling³⁸. The rate depends strongly on the charging energy difference \tilde{E} , before and after the process, which in the present problem depends on the quantum state $|0\rangle$ of the qubit via $E_0^N - E_0^{N+1}$. At finite temperatures the step-function is replaced by $\Theta(E) \rightarrow [1 - \exp(-E/k_B T)]^{-1}$.

Similar expressions can be derived for the other tunneling processes in the left and right junction, increasing or decreasing the island charge, N (and m accordingly). If the temperature is low and the applied transport voltage not too high we can concentrate on two adjacent charge states of the SET transistor, say $N = 0$ and $N = 1$. (To avoid confusion with the states of the qubit we will keep using the notation N and $N + 1$.) Thus, only two tunneling processes, in forward direction as defined by the transport voltage, take place. These are the transitions $N, m \rightarrow N + 1, m$ through the left junction and $N + 1, m \rightarrow N, m + 1$ through the right junction. (It is clear that the SET has to be driven by a sufficient transport voltage that both processes have nonzero rates for any state of the qubit.) Hence we need to consider five additional ‘in’ rates

$$\begin{aligned} \Sigma_{1,N,m \rightarrow 1,N+1,m}^{1,N,m \rightarrow 1,N+1,m}(\Delta t) &\approx \Gamma_{L,1} \delta(\Delta t), \\ \Sigma_{1,N,m \rightarrow 1,N+1,m}^{0,N,m \rightarrow 0,N+1,m}(\Delta t) &\approx \Gamma_L \delta(\Delta t), \\ \Sigma_{0,N+1,m \rightarrow 0,N,m+1}^{0,N+1,m \rightarrow 0,N,m+1}(\Delta t) &\approx \Gamma_{R,0} \delta(\Delta t), \\ \Sigma_{1,N+1,m \rightarrow 1,N,m+1}^{1,N+1,m \rightarrow 1,N,m+1}(\Delta t) &\approx \Gamma_{R,1} \delta(\Delta t), \\ \Sigma_{1,N+1,m \rightarrow 1,N,m+1}^{0,N+1,m \rightarrow 0,N,m+1}(\Delta t) &\approx \Gamma_R \delta(\Delta t) \end{aligned} \quad (44)$$

and their ‘out’ counterparts with opposite signs.

The rates introduced above can be expressed as follows

$$\begin{aligned} \Gamma_L &\equiv 2\pi\alpha_L [\mu_L - E_{\text{set}}(1 - 2N_{\text{set}})], \\ \Gamma_R &\equiv 2\pi\alpha_R [-\mu_R + E_{\text{set}}(1 - 2N_{\text{set}})] \end{aligned} \quad (45)$$

and

$$\begin{aligned} \Gamma_{L,0} &\equiv \Gamma_L + \Delta\Gamma_L, \\ \Gamma_{L,1} &\equiv \Gamma_L - \Delta\Gamma_L, \\ \Gamma_{R,0} &\equiv \Gamma_R + \Delta\Gamma_R, \\ \Gamma_{R,1} &\equiv \Gamma_R - \Delta\Gamma_R. \end{aligned} \quad (46)$$

The shifts are proportional to the difference in the qubit’s energy as a result of the transition,

$$\begin{aligned} \Delta\Gamma_L &\equiv \pi\alpha_L(\Delta E_{\eta}^{N+1} - \Delta E_{\eta}^N), \\ \Delta\Gamma_R &\equiv -\pi\alpha_R(\Delta E_{\eta}^{N+1} - \Delta E_{\eta}^N). \end{aligned} \quad (47)$$

As we will see, these shifts are responsible for the separation of the peaks of $P(m, t)$.

We, furthermore, analyze transitions due to single electron tunneling where the qubit changes its state, i.e. the mixing transitions. As explained above, we evaluate the rates for these processes in linear order in ϵ_N . They are

$$\begin{aligned}\Sigma_{1,N,m \rightarrow 0,N+1,m}^{0,N,m \rightarrow 0,N+1,m}(\Delta t) &\approx \frac{\omega_L}{2}\delta(\Delta t), \\ \Sigma_{1,N+1,m \rightarrow 0,N,m+1}^{0,N+1,m \rightarrow 0,N,m+1}(\Delta t) &\approx -\frac{\omega_R}{2}\delta(\Delta t), \\ \Sigma_{1,N,m \rightarrow 1,N+1,m}^{0,N,m \rightarrow 1,N+1,m}(\Delta t) &\approx \frac{\omega_L}{2}\delta(\Delta t), \\ \Sigma_{1,N+1,m \rightarrow 1,N,m+1}^{0,N+1,m \rightarrow 1,N,m+1}(\Delta t) &\approx -\frac{\omega_R}{2}\delta(\Delta t), \\ \Sigma_{0,N,m \rightarrow 1,N+1,m}^{0,N,m \rightarrow 1,N+1,m}(\Delta t) &\approx \frac{\omega_L}{2}\delta(\Delta t), \\ \Sigma_{0,N+1,m \rightarrow 1,N,m+1}^{0,N+1,m \rightarrow 1,N,m+1}(\Delta t) &\approx -\frac{\omega_R}{2}\delta(\Delta t), \\ \Sigma_{1,N,m \rightarrow 0,N+1,m}^{1,N,m \rightarrow 0,N+1,m}(\Delta t) &\approx -\frac{\omega_L}{2}\delta(\Delta t), \\ \Sigma_{1,N+1,m \rightarrow 0,N,m+1}^{1,N+1,m \rightarrow 0,N,m+1}(\Delta t) &\approx \frac{\omega_R}{2}\delta(\Delta t).\end{aligned}$$

Again their “out” counterparts differ in the sign. Here $\omega_{L,R} \equiv \pi\alpha_{L,R}\Delta E_\eta^{N+1}\epsilon_{N+1}$ is proportional to the energy difference of the two qubit’s states if the SET island is in the nonequilibrium state $N+1$.

The master equation to be analyzed thus becomes:

$$\frac{d\hat{\sigma}(t)}{dt} - \frac{i}{\hbar}[\hat{\sigma}(t), H_0] = \hat{\Gamma}\hat{\sigma}(t) + \hat{\omega}\hat{\sigma}(t), \quad (48)$$

where $\hat{\Gamma}$ is the matrix formed by the transition rate obtained in zeroth order in ϵ_N and $\hat{\omega}$ is the matrix of the rates linear in ϵ_N .

As mentioned before, we only need to consider the matrix elements $\hat{\sigma}_{i,j}^{N,m} \equiv \hat{\sigma}_{j,N,m}^{i,N,m}$ of the density matrix which are diagonal in the SET degrees of freedom. To proceed we perform a Fourier transform with respect to m , $\hat{\sigma}_{i,j}^N(k) \equiv \sum_m \hat{\sigma}_{i,j}^{N,m} e^{ikm}$. To shorten formulas we introduce $A^N \equiv \hat{\sigma}_{0,0}^N(k)$, $B^N \equiv \hat{\sigma}_{1,1}^N(k)$, $C^N \equiv \sum_m \text{Re } \hat{\sigma}_{0,1}^{N,m} e^{ikm}$, and $D^N \equiv \sum_m \text{Im } \hat{\sigma}_{0,1}^{N,m} e^{ikm}$. This enables us to rewrite (48) as:

$$\begin{aligned}\dot{A}^N &= -\Gamma_{L,0}A^N + \Gamma_{R,0}e^{ik}A^{N+1} \\ &\quad - \omega_L C^N - \omega_R e^{ik}C^{N+1},\end{aligned} \quad (49)$$

$$\begin{aligned}\dot{A}^{N+1} &= \Gamma_{L,0}A^N - \Gamma_{R,0}A^{N+1} - \Omega D^{N+1} \\ &\quad + \omega_L C^N + \omega_R C^{N+1},\end{aligned} \quad (50)$$

$$\begin{aligned}\dot{B}^N &= -\Gamma_{L,1}B^N + \Gamma_{R,1}e^{ik}B^{N+1} \\ &\quad - \omega_L C^N - \omega_R e^{ik}C^{N+1},\end{aligned} \quad (51)$$

$$\begin{aligned}\dot{B}^{N+1} &= \Gamma_{L,1}B^N - \Gamma_{R,1}B^{N+1} + \Omega D^{N+1} \\ &\quad + \omega_L C^N + \omega_R C^{N+1},\end{aligned} \quad (52)$$

$$\begin{aligned}\dot{C}^N &= -\Delta E_\eta^N D^N - \Gamma_L C^N + \Gamma_R e^{ik}C^{N+1} \\ &\quad - \frac{\omega_L}{2}(A^N - B^N) - \frac{\omega_R}{2}e^{ik}(A^{N+1} - B^{N+1}),\end{aligned} \quad (53)$$

$$\dot{C}^{N+1} = -\Delta E_\eta^{N+1} D^{N+1} + \Gamma_L C^N - \Gamma_R C^{N+1}$$

$$+ \frac{\omega_L}{2}(A^N - B^N) + \frac{\omega_R}{2}(A^{N+1} - B^{N+1}), \quad (54)$$

$$\dot{D}^N = \Delta E_\eta^N C^N - \Gamma_L D^N + \Gamma_R e^{ik}D^{N+1}, \quad (55)$$

$$\begin{aligned}\dot{D}^{N+1} &= \Delta E_\eta^{N+1} C^{N+1} + \Gamma_L D^N - \Gamma_R D^{N+1} \\ &\quad + \frac{\Omega}{2}(A^{N+1} - B^{N+1}).\end{aligned} \quad (56)$$

Here $\Omega \equiv 2E_{\text{int}} \sin \eta$ is the coefficient in the mixing term in H_{int} for $N = 1$ (see (32)). The terms proportional to ΔE_η^N and Ω originate from the coherent left hand side of (48).

C. Qualitative analysis of the master equation

First, we analyze the system (49)–(56) qualitatively. Imagine that we can “switch off” the Josephson coupling in the qubit during the measurement. Then all the mixing terms in (49)–(56), i.e. those proportional to Ω and $\omega_{L,R}$ disappear, and the system factorizes into three independent groups. The first one (49,50),

$$\begin{aligned}\dot{A}^N &= -\Gamma_{L,0}A^N + \Gamma_{R,0}e^{ik}A^{N+1}, \\ \dot{A}^{N+1} &= \Gamma_{L,0}A^N - \Gamma_{R,0}A^{N+1},\end{aligned} \quad (57)$$

has exponential solutions $\propto e^{i\omega t}$ and eigenvalues

$$\omega_{1,2} = \frac{i}{2}(\Gamma_{L,0} + \Gamma_{R,0}) \left\{ 1 \pm \left[1 + \frac{4\Gamma_0(e^{ik} - 1)}{\Gamma_{L,0} + \Gamma_{R,0}} \right]^{\frac{1}{2}} \right\}. \quad (58)$$

Here

$$\Gamma_0 \equiv \frac{\Gamma_{L,0}\Gamma_{R,0}}{\Gamma_{L,0} + \Gamma_{R,0}} \quad (59)$$

is the rate for single-electron tunneling through the SET if the qubit in the state $|0\rangle$. When k is small the first eigenvalue, $\omega_1 \approx i(\Gamma_{L,0} + \Gamma_{R,0})$, is large and the corresponding eigenvector quickly dies out. The second eigenvalue $\omega_2 \approx \Gamma_0 k + i\Gamma_0 c_0 k^2$ is small, and the corresponding eigenvector, with $A^{N+1}/A^N = \Gamma_{L,0}/\Gamma_{R,0}$, survives. This solution describes a wave packet propagating with the group velocity Γ_0 , which widens due to shot noise of the single electron tunneling, its width being given by $\sqrt{\Gamma_0 c_0 t}$. The factor $c_0 \equiv (\Gamma_{L,0}^2 + \Gamma_{R,0}^2)/(\Gamma_{L,0} + \Gamma_{R,0})^2$ varies between 1/2 in the symmetric situation ($\Gamma_{L,0} = \Gamma_{R,0}$) and 1 in the extremely asymmetric case ($\Gamma_{L,0}$ much larger or much smaller than $\Gamma_{R,0}$).

Analogously the second group of equations (51,52) for B^N and B^{N+1} describe a wave packet which moves in m -direction with group velocity

$$\Gamma_1 \equiv \frac{\Gamma_{L,1}\Gamma_{R,1}}{\Gamma_{L,1} + \Gamma_{R,1}} \quad (60)$$

and width growing as $\sqrt{\Gamma_1 c_1 t}$. The two peaks correspond to the qubit in the states $|0\rangle$ and $|1\rangle$, respectively. They

separate when their distance is larger than their widths, i.e. $|\Gamma_0 - \Gamma_1|t \geq \sqrt{\Gamma_0 c_0}t + \sqrt{\Gamma_1 c_1}t$. This means that after the time

$$t_{\text{ms}} \equiv \left(\frac{\sqrt{\Gamma_0 c_0} + \sqrt{\Gamma_1 c_1}}{|\Gamma_0 - \Gamma_1|} \right)^2, \quad (61)$$

which we denote as the measurement time, the process can constitute a quantum measurement.

To get a clue for the dephasing we analyze the third group of equations (53)–(56) at $k = 0$ (which is equivalent to a trace over m). The four equations may be recombined into two complex ones:

$$\begin{aligned} \frac{d}{dt} \hat{\sigma}_{0,1}^N(0) &= i\Delta E_\eta^N \hat{\sigma}_{0,1}^N(0) - \Gamma_L \hat{\sigma}_{0,1}^N(0) + \Gamma_R \hat{\sigma}_{0,1}^{N+1}(0) \\ \frac{d}{dt} \hat{\sigma}_{0,1}^{N+1}(0) &= i\Delta E_\eta^{N+1} \hat{\sigma}_{0,1}^{N+1}(0) + \Gamma_L \hat{\sigma}_{0,1}^N(0) - \Gamma_R \hat{\sigma}_{0,1}^{N+1}(0) \end{aligned} \quad (62)$$

The analysis of this set shows that if $dE \equiv |\Delta E_\eta^{N+1} - \Delta E_\eta^N| \approx 2E_{\text{int}} \ll (\Gamma_L + \Gamma_R)$ the imaginary parts of the eigenvalues are $\text{Im } \omega_1 \approx (\Gamma_L + \Gamma_R)$ and $\text{Im } \omega_2 \approx \frac{dE^2}{4(\Gamma_L + \Gamma_R)}$. In the opposite limit $dE \gg (\Gamma_L + \Gamma_R)$ the imaginary parts are $\text{Im } \omega_1 \approx \Gamma_L$ and $\text{Im } \omega_2 \approx \Gamma_R$. The first limit is physically more relevant (we have assumed parameters in this regime), although the second one is also possible if the tunneling is very weak or the coupling between the qubit and the SET transistor is strong. In both limits the dephasing time, which is defined as the the longer of the two times,

$$\tau_\phi \equiv \max\{[\text{Im } \omega_1]^{-1}, [\text{Im } \omega_2]^{-1}\} \quad (63)$$

is parametrically different from the measurement time (61). In the first limit, $dE \ll (\Gamma_L + \Gamma_R)$, it is

$$\tau_\phi = \frac{4(\Gamma_L + \Gamma_R)}{(dE)^2} \approx \frac{\Gamma_L + \Gamma_R}{E_{\text{int}}^2}. \quad (64)$$

One can check that in the whole range of validity of our approach the measurement time exceeds the dephasing time, $t_{\text{ms}} > \tau_\phi$. This is consistent with the fact that a “good” quantum measurement should completely dephase a quantum state.

The reason for the difference between the measurement time and the dephasing time is the entanglement of the qubit’s state with the additional microscopic states of the SET, — the states which cannot be characterized by the number of electrons which have tunneled through the transistor, m , only. Imagine that we know (with high probability) that during some time from the beginning of the measurement process exactly one electron has tunneled through the SET whatever the qubit’s state was. Does it mean that with that high probability there was no dephasing? The answer is no. The transport of electrons occurs via a real state of the island, $N + 1$. The system may spend different times in this intermediate

state, i.e. different phase shifts are acquired between the two states of the qubit. Since the time spent in the state $N + 1$ is actually random, some dephasing has occurred. Next we can ask where the information about this phase uncertainty is stored, i.e. which states has the qubit become entangled with. These may not be the states with different m or N since m is equal to one and N is again equal to zero irrespective of the state of the qubit. The only possibility are the microscopic states of the middle island and/or leads, which were subject to different time evolutions during different histories of the tunneling process. To put it in the language of Ref. 39, the initial state of the system $(a|0\rangle + b|1\rangle)|\chi\rangle|m = 0\rangle$ evolves into $a|0\rangle|\chi_0\rangle|m_0\rangle + b|1\rangle|\chi_1\rangle|m_1\rangle$, where $|\chi\rangle$ stands for the quantum state of the uncontrolled environment. One may imagine a situation when $m_0 = m_1$, but $|\chi_0\rangle$ and $|\chi_1\rangle$ are orthogonal. In this situation the dephasing has occurred but no measurement has been performed.

In Refs. 19–21, a quantum point contact (QPC) measuring device was used only as a source of dephasing, i.e. the information on the current flowing in the measuring device was disregarded. Thus a distinction between measurement and dephasing was not made. However the expressions for the dephasing time were given by expressions similar to (61). As it became clear later^{40,41}, the QPC does not involve an additional uncontrolled environment during the measurement process and, therefore, $t_{\text{ms}} = \tau_\phi$. Indeed, the tunneling in the QPC does not occur via a real intermediate state and the discussion above does not apply. In this sense the QPC may be regarded as a 100% efficient measuring device. The additional environment in the SET, which, as mentioned, reduces the efficiency of the measuring device, plays, actually, a positive role in the quantum measurement, provided it dephases the state of the qubit only when the system is driven out of equilibrium. This is because the quicker dephasing suppresses the transitions between the states of the qubit (such a suppression of the transitions due to a continuous observation of the quantum state of the system is called the Zeno effect)⁴¹, while the initial probabilities are preserved. It is worth noting that our system might also be used as a 100% efficient device, if it was biased in the co-tunneling regime. However, this possibility has other drawbacks.

D. The mixing time

Finally, we analyze what happens if we take into account the mixing terms in the system (49)–(56). We consider $k = 0$ and investigate the eigenvalues of the eight by eight matrix formed by the coefficients of (49)–(56). Note that in the discussion above we have calculated all the eight eigenvalues for $E_J = 0$ (the two eigenvalues of the complex system (62) are doubled when one considers it as a system of four real equations). In the diagonal part there were two zeros, which corresponded to two con-

served quantities (for $k = 0$), $A^N(0) + A^{N+1}(0) = \hat{\sigma}_{0,0}$ and $B^N(0) + B^{N+1}(0) = \hat{\sigma}_{1,1}$. Six other eigenvalues were large compared to the amplitudes of the mixing terms. It is clear, that including the mixing, $E_J \neq 0$, changes only slightly the values of the six large eigenvalues. Moreover, one of the eigenvalues is always zero. This corresponds to the conservation of the total trace $A^N(0) + A^{N+1}(0) + B^N(0) + B^{N+1}(0) = 1$. The last (8th) eigenvalue acquires now a small imaginary part and this gives the time scale of the mixing between the two states of the qubit.

We can estimate the value of the mixing time for a concrete physical situation. We assume $\alpha_L = \alpha_R \equiv \alpha$. We choose N_{set} far enough from the degeneracy point, which is $N_{\text{set}} = 1/2$, so that $\Gamma_L < \Gamma_R$ and the related Coulomb blockade energy, $E_{\text{CB}} \equiv E_{\text{set}}(1 - 2N_{\text{set}})$, is of the order of E_{set} . To satisfy the conditions for the Golden Rule (see (40) and the discussion thereafter) we assume E_{CB} to be the largest energy scale of the system, $E_{\text{CB}} \gg \Delta E$ ($\Delta E \equiv \Delta E_\eta$ is the qubit's energy level splitting), and the chemical potential of the left lead $\mu_L = V_{\text{tr}}/2$ to exceed the Coulomb blockade energy by an amount of the order of E_{CB} . The transport voltage should not exceed the value, beyond which further charge states of the SET transistor, e.g. $N+2$ and $N-1$, become involved. Thus $V_{\text{tr}}/2 < E_{\text{set}}(1 + 2N_{\text{set}})$ and N_{set} should be chosen far enough from zero as well. In this regime we estimate the mixing time as

$$t_{\text{mix}}^{-1} \approx \frac{2\pi\alpha}{\hbar} \frac{E_{\text{int}}^2 E_J^2}{(\Delta E)^4} E_{\text{set}}. \quad (65)$$

The measurement time in the same regime is given approximately by

$$t_{\text{ms}}^{-1} \approx \frac{2\pi\alpha}{\hbar} \frac{E_{\text{int}}^2}{E_{\text{set}}}. \quad (66)$$

For comparison we also give a rough value for the dephasing time, which is short when the measurement is performed. We assume the regime in which Eq. (64) is valid. Then

$$\tau_\phi^{-1} \approx \frac{1}{2\pi\alpha\hbar} \frac{E_{\text{int}}^2}{E_{\text{set}}}. \quad (67)$$

Note that the limit $\alpha \rightarrow 0$ is not allowed in (67), since the validity of (64) eventually breaks down in this limit.

The precise values of N_{set} and V_{tr} determine the numerical coefficients in the previous expressions. Thus, $t_{\text{ms}}/t_{\text{mix}} \propto E_J^2 E_{\text{set}}^2 / (\Delta E)^4$. One recognizes two competing ratios here: $E_J/\Delta E$, which is small, and $E_{\text{set}}/\Delta E$, which is large. The condition $t_{\text{ms}}/t_{\text{mix}} \ll 1$, thus, imposes an additional constraint on the parameters of the system. On the other hand, for low conductance barriers in the SET ($\alpha < 1$ but not too small), the dephasing time is always shorter than the measurement time.

E. Discussion and Extensions

Let us summarize what has been done thus far: To measure the quantum state of the qubit we attach a SET to the qubit and describe the time evolution of the whole system. We, then, find two complimentary descriptions of the measurement process. In the first we trace over the SET's degrees of freedom and obtain a reduced density matrix of the qubit. From the time evolution of the last we deduce the dephasing time and the mixing time, i. e. the relaxation times for the off-diagonal and the diagonal elements of the reduced density matrix respectively. This information does not, however, predict the results of the measurement of the current in the SET. Therefore, in a second description, we calculate the probability distribution, $P(m, t)$, of the number of electrons m which have passed through the SET during time t . We have evaluated $P(m, t)$ numerically for parameters to be specified in the next section. The results, shown in Fig. 8 and 9, display the time evolution on the time scale of t_{ms} , relevant for the measurement process.

We observe that under appropriate conditions $P(m, t)$ splits into two separate peaks, whose weights are given by the initial probabilities of the logical states of the qubit. The splitting time is the minimum time after which one can distinguish between the states of the qubit and we call it, therefore, the measurement time, t_{ms} . The measurement time turns out to be longer than the dephasing time. This fact indicates that in our case some additional part of the environment “observes” the state of the qubit during the measurement⁴⁰.

Note, that the knowledge of $P(m, t)$ does not provide immediately the value of the current flowing in the SET at all times. Recently, attempts have been made to describe the measurement process in terms of the current in the measuring device^{40,42}. However, as was discussed in Ref. 41, this approach may be misleading. The author of Ref. 41 addresses also the long time behavior of this current ($t > t_{\text{mix}}$) and finds that it will strongly depend on whether “real” (a la von Neumann) collapses of the wave function take place along with the continuous measurement process. Thus, further investigation of this problem is definitely needed.

FIG. 9. $P(m,t)$, the probability that m electrons have tunneled during time t . The parameters are those given in the text, $E_J = 0.25\text{K}$. The time is measured in nanoseconds. The initial amplitudes of the qubit's states: $a = \sqrt{0.75}$, $b = \sqrt{0.25}$.

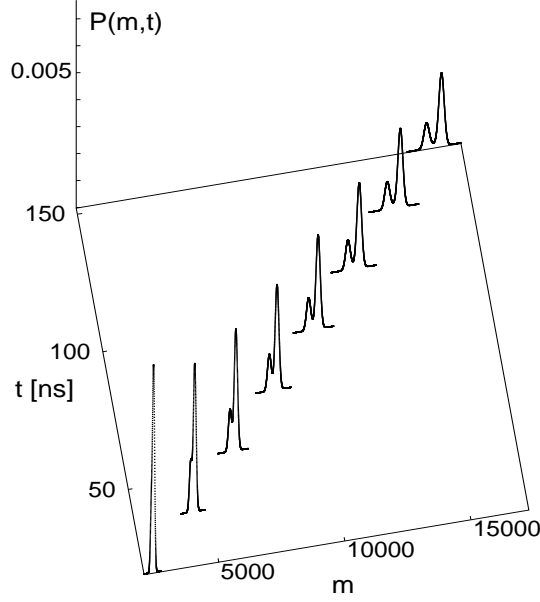
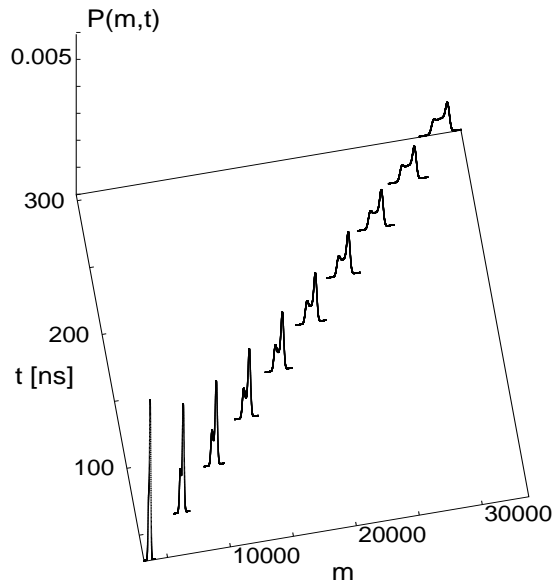


FIG. 8. $P(m,t)$, the probability that m electrons have tunneled during time t . The parameters are those given in the text, $E_J = 0.1\text{K}$. The time is measured in nanoseconds. The initial amplitudes of the qubit's states: $a = \sqrt{0.75}$, $b = \sqrt{0.25}$.



V. DISCUSSION

A. Choice of parameters

To demonstrate that the constraints on the circuit parameters can be met by available technology, we summarize the constraints and suggest a suitable set. The necessary conditions are: $\Delta > E_{qb} \gg E_J, E_L, k_B T$. The temperature has to be chosen low to assure the initial thermalization, $k_B T \ll E_{qb}$ and $k_B T \ll \hbar\omega_{LC}$, and to reduce the dephasing effects. A good choice is $k_B T \sim E_J/2$ since further cooling would not decrease the dephasing rate at the degeneracy point much further. Then, the dephasing rates during operations (at the degeneracy point) and in the idle state (off degeneracy) are close to each other.

Depending on the parameters chosen, the number of qubits N and the total computation time are restricted. The dephasing times limits the number of operations to $\tau_{op} \ll \Gamma_{in}^{-1}, \Gamma_{\phi}^{-1}$. This is the only restriction for a single qubit. If several qubits are coupled, the dephasing for the whole system is faster. Since the sources of dissipation for different qubits are independent, the dephasing time gets N times shorter. In addition, the energy splittings of the qubits should fit into the range provided by Eq. (9), and the levels within this range should be sufficiently different from each other to minimize the errors introduced by non-zero inter-qubit coupling between 2-bit operations (cf. Section II). As shown in Appendix B, this provides a restriction on the number of qubits and the number of operations which can be performed: the number of 2-bit gates is limited to $4N^{-4}(\hbar\omega_{LC}^{(N=1)}/E_L)^2$ and the number of single-bit gates to the same amount or, if it is larger, to $8N^{-1}(E_J/E_L)^2$. With circuit parameters discussed below and for not too many qubits (\leq several tens) these restrictions are weaker than those provided by the dephasing. Moreover, we note that these restrictions are removed if the interaction is effectively turned off. This can be achieved on the “software” level, by the use of refocusing voltage pulses. On the “hardware” level this is achieved with the improved design suggested in Ref. 17. This allows for larger numbers of qubits and longer computations.

As an example we suggest a system with the following parameters:

(i) We choose junctions with the capacitance $C_J = 4 \cdot 10^{-16}\text{F}$, corresponding to the charging energy (in temperature units) $E_{qb} \sim 2\text{K}$, and a smaller gate capacitance $C = 2.5 \cdot 10^{-18}\text{F}$ to reduce the coupling to the environment. Thus at the working temperature of $T = 50\text{mK}$ the initial thermalization is assured. The superconducting gap has to be slightly larger $\Delta > E_{qb}$. We further

choose $E_J = 100\text{mK}$, i.e. the time scale of one-qubit operations is $\tau_{\text{op}}^{(1)} = \hbar/E_J \sim 7 \cdot 10^{-11}\text{s}$.

(ii) We assume that the resistor in the gate voltages circuit has $R \sim 50\Omega$. Voltage fluctuations limit the dephasing time (23). We thus arrive at an estimate of the decoherence rate which allows for $(\Gamma_\phi \tau_{\text{op}}^{(1)})^{-1} \sim 8 \cdot 10^5$ coherent operations for a single bit.

(iii) To assure sufficiently fast 2-bit operations we choose $L \sim 3\mu\text{H}$. Then, the decoherence time is $(\Gamma_\phi \tau_{\text{op}}^{(2)})^{-1} \sim 650$ times longer than a 2-bit operation.

In Table I we present alternative sets of parameters, assuming throughout that the resistance is fixed to be $R = 50\Omega$.

TABLE I. Examples of suitable sets of parameters.

C (aF)	C_J (aF)	E_J (mK)	T (mK)	L (μH)	1-bit oper-s	2-bit oper-s
2.5	400	100	50	3	$8 \cdot 10^5$	650
2.5	400	250	125	1	$8 \cdot 10^5$	500
2.5	400	250	125	3	$8 \cdot 10^5$	1600
40	400	40	20	1	$4 \cdot 10^3$	85
10	400	100	50	1	$5 \cdot 10^4$	200
40	400	100	50	0.5	$4 \cdot 10^3$	100

The quantum measurement process introduces additional constraints on the parameters. In order to demonstrate that the conditions assumed in this paper are realistic we chose the charging energies E_{set} , E_{qb} and E_{int} as follows: The capacitance of the Josephson junction is $C_J = 4.0 \cdot 10^{-16}\text{F}$, the gate capacitance of the qubit $C = 2.5 \cdot 10^{-18}\text{F}$, the capacitances of the normal tunnel junctions of the SET $C' = 2.0 \cdot 10^{-17}\text{F}$, the gate capacitance of the SET $C_g = 2.5 \cdot 10^{-18}\text{F}$, and the capacitance between the SET and the qubit $C_{\text{int}} = 2.5 \cdot 10^{-18}\text{F}$. We obtain: $E_{\text{set}} \approx 20\text{K}$, $E_{\text{qb}} \approx 2.5\text{K}$, $E_{\text{int}} \approx 0.25\text{K}$. Taking $n_{\text{qb}} = 0.35$, $N_{\text{set}} = 0.15$ and $eV_{\text{tr}} = 48\text{K}$ we get $\Delta E \approx 3\text{K}$, $E_{\text{CB}} \equiv E_{\text{set}}(1 - 2N_{\text{set}}) \approx 14\text{K}$, and $V_{\text{tr}}/2 - E_{\text{CB}} \approx 10\text{K}$ (for definitions see subsection IV D). We also assume $2\pi\alpha = 0.1$. The measurement time in this regime is $t_{\text{ms}} \approx 0.25 \cdot 10^4\hbar/(k_B 1\text{K}) \approx 1.8 \cdot 10^{-8}\text{s}$. For this choice of parameters we calculate t_{mix} numerically, assuming first $E_J = 0.1\text{K}$, and we obtain $t_{\text{mix}} \approx 1.4 \cdot 10^5\hbar/(k_B 1\text{K}) \approx 1.0 \cdot 10^{-6}\text{s}$. Thus $t_{\text{mix}}/t_{\text{ms}} \approx 55$ and the separation of peaks should occur much earlier than the transitions happen. Indeed, the numerical simulation of the system (49)–(56) for those parameters given above shows almost ideal separation of peaks (see Fig. 8). On the other hand, for $E_J = 0.25\text{K}$, and we obtain $t_{\text{mix}}/t_{\text{ms}} \approx 9$. This is a marginal situation. The numerical simulation in this case (see Fig. 9) shows that the peaks, first, start to separate, but, later, the valley between the peaks is filled due to the mixing transitions.

These numbers demonstrate that the quantum manipulations of Josephson junction qubits, as discussed in this paper, can be tested experimentally using the currently available lithographic and cryogenic techniques. We have further demonstrated that the current through a single-electron transistor can serve as a measurement of the quantum state of the qubit, in the sense that in the case of a superposition of two eigenstates it gives one or the other result with the appropriate probabilities.

B. Comparison with existing experiments

The demonstration that the qubit is in a superposition of eigenstates should be distinguished from another question, namely whether it is possible to verify that an eigenstate of a qubit is actually a superposition of two different charge states, which depends on the mixing angle η as described by Eq. (31). This question has been addressed in the experiments of Ref. 11. They used a setup similar to the one shown in Fig. 4, a single-Cooper-pair box coupled to a single-electron transistor. They could demonstrate that the expectation value of the charge in the box varies continuously as a function of the applied gate voltage as follows from (31). Another experiment along the same lines has been performed by Nakamura et al.¹⁵. They demonstrated by spectroscopy that the energy of the ground state and of the first excited state have the expected gate-voltage dependence of superpositions of charge states.

Our theory can also describe the type of measurements performed in Ref. 11. For this purpose we analyze the rates in the master equation (48) for general values of the mixing angle η , relaxing the requirement $\tan \eta \ll 1$. Then, for our approach to be valid, we must have $E_{\text{int}} \ll E_J$, so that $\tan \epsilon_N \ll 1$. In this regime each eigenstate of the qubit, $|0\rangle$ or $|1\rangle$, corresponds to a single, though η -dependent propagation velocity (Γ_0 or Γ_1). Thus, if the qubit is prepared in one of its eigenstates, then even at the degeneracy point ($\eta = \pi/2$) where the eigenstates are equally weighted superpositions of two charge states, one would observe only one peak. We have calculated Γ_0 as a function of η using (45), (46), (47), and (59) and obtained curves (not shown here) very similar to those in the experiments. It should be added that near degeneracy our setup would not be efficient in projecting onto the eigenstates anymore, since the difference between the velocities of the peaks, $|\Gamma_0 - \Gamma_1|$, vanishes near the degeneracy point.

C. Related theories

It is also interesting to compare our proposal with the “quantum jumps” technique employed in quantum optics in general, and with the realizations of the qubits by trapped ions in particular (for a review see Ref. 43). Indeed, the concepts are very close in spirit: the state of the system is examined by an external nonequilibrium current (electrons in our case and photons in the quantum jumps technique). There is, however, an important difference. In the quantum jumps measurements only one of the logical states scatters photons. Therefore, the efficiency of the measurement is limited by the ability to detect photons. In principle we could realize this situation also in our system, if we bias the SET transistor such that different states of the qubit switch the transistor between the off and on regimes. Then the efficiency

of the measurement is determined by the ability to detect individual electron — which is possible in single-electron devices, for instance by charging a single-electron box — and the measurement time would be given by the time it takes the first electron to tunnel. However, this mode of operation would require that the SET transistor is kept near the switching point, where thermal fluctuations and higher order processes could modify the picture substantially. Therefore, we have concentrated here on a situation in which the SET transistor conducts for both states of the qubit, and the measurement requires distinguishing large numbers of charges or macroscopic currents. Accordingly, the measurement time is limited by the shot noise. Another, less important difference is that in our system there is no third state of the qubit, which resonates with only one of the logical states. Therefore, the qubit is restricted to stay always in the two dimensional Hilbert space.

D. Summary

To conclude, the fabrication of Josephson junction qubits is possible with current technology. In these systems fundamental features of macroscopic quantum-mechanical systems can be explored. More elaborate designs as well as further progress of nano-technology, will provide longer coherence times and allow scaling to larger numbers of qubits. The application of Josephson junction systems as elements of a quantum computer, i.e. with a very large number of manipulations and large number of qubits, will remain a challenging issue, demanding in addition to the perfect control of time-dependent gate voltages a still longer phase coherence time. We stress, however, that many aspects of quantum information processing can initially be tested on simple circuits as proposed here.

We have further shown that a single-electron transistor capacitively coupled to a qubit may serve as a quantum measuring device in an accessible range of parameters. We have described the process of measurement by deriving the time evolution of the reduced density matrix. We found that the dephasing time is shorter than the measurement time, and we have estimated the mixing time, i.e. the time scale on which the transitions induced by the measurement occur.

ACKNOWLEDGMENTS

We thank E. Ben-Jacob, T. Beth, C. Bruder, L. Dreher, Y. Gefen, Z. Hermon, J. König, Y. Levinson, J. E. Mooij, T. Pohjola, and H. Schoeller for stimulating discussions. This work has been supported by a Graduiertenkolleg and the SFB 195 of the DFG, the A. v. Humboldt foundation (Y.M.) and the German Israeli Foundation (Contract G-464-247.07/95) (A.S.).

APPENDIX A:

The form of the master equation (36) suggests the use of a Laplace transformation, after which the last term in (36) becomes $\Sigma(s)\hat{\sigma}(s)$. We Laplace transform (40) in the regime $s \ll \tilde{E}$, i.e. we assume the density matrix $\hat{\sigma}$ to change slowly on the time scale given by \hbar/\tilde{E} . This assumption should be verified later for self-consistency. At zero temperature ($\beta \rightarrow \infty$) and for $\delta \rightarrow 0$ we obtain:

$$\begin{aligned} & \Sigma_{N,m,0 \rightarrow N+1,m,0}^{N,m,0 \rightarrow N+1,m,0}(s) \\ &= 2\alpha_L \text{Re} \left[(s + i\tilde{E}) e^{i\delta(s+i\tilde{E})} E_1[i\delta(s+i\tilde{E})] \right] \\ & \approx 2\pi\alpha_L \tilde{E} \Theta(\tilde{E}) - 2\alpha_L s(1 + \gamma + \ln(|\tilde{E}\delta|)) , \end{aligned} \quad (\text{A1})$$

where $E_1[\dots]$ is the exponential integral and $\gamma \approx 0.58$ is Euler's constant. Denoting the diverging factor $[1 + \gamma + \ln(|\tilde{E}\delta|)]$ by $D(\tilde{E})$ and performing the inverse Laplace transform we arrive at

$$\begin{aligned} & \Sigma_{0,N,m \rightarrow 0,N+1,m}^{0,N,m \rightarrow 0,N+1,m}(\Delta t) \\ & \approx 2\pi\alpha_L \tilde{E} \Theta(\tilde{E}) \delta(\Delta t + 0) - 2\alpha_L D(\tilde{E}) \delta'(\Delta t + 0) . \end{aligned} \quad (\text{A2})$$

Note that (A2) is equivalent to (40) only as a kernel in the convolution (36) when applied to slowly changing matrix elements of $\hat{\sigma}$. The first term of (A2) is the usual Golden Rule tunneling rate corrected with respect to the additional charging energy corresponding to the quantum state $|0\rangle$ of the qubit, $E_0^N - E_0^{N+1}$. The second (diverging) part of (A2) produces a term proportional to $\frac{d}{dt} \hat{\sigma}_{N,m,0}^{N,m,0}$. One can take this term to the LHS of (36) so that the time derivative in the LHS will look like $\frac{d}{dt} [\hat{\sigma}_{0,0}^{N+1,m} - 2\alpha_L D(\tilde{E}) \hat{\sigma}_{0,0}^{N,m}]$. We analyzed all possible choices of the qubit's indices in Figs. 6,7 and arrived at the conclusion that the diverging terms have always the same structure as the coherent terms in the LHS of (36). Moreover, if we neglect some energy corrections of order E_{int} , we may incorporate all of these terms to the LHS of (36), so that the master equation reads:

$$(1 + \alpha_L A + \alpha_R B) \left[\frac{d\hat{\sigma}(t)}{dt} - \frac{i}{\hbar} [\hat{\sigma}(t), H_0] \right] = \Sigma_{\text{reg}} \hat{\sigma}(t) , \quad (\text{A3})$$

where A and B are tri-diagonal matrices in the N and m spaces, composed of the diverging factors of the type of $D(\tilde{E})$, while Σ_{reg} is the regular local part of $\Sigma(t-t')$.

We expect that without the approximation of energies in the diverging terms the structure of (A3) would be

the same, with A and B being more complicated matrices, which would include some mixing in the space of the qubit's states. Finally, we note that for any physically reasonable choice of the cut-off δ , the logarithmically divergent factors in the matrices A and B are of order one, and, therefore, the mixing corrections to the unit matrix in the LHS of (A3) are small. We multiply the master equation (A3) by $(1 + \alpha_L A + \alpha_R B)^{-1} \approx (1 - \alpha_L A - \alpha_R B)$ from the left, so that the mixing corrections move to the RHS. Since Γ is linear in α_L and α_R , the mixing corrections are quadratic. We drop them in the framework of the first order perturbation theory.

APPENDIX B:

Our prescription for 2-bit operations, as described in subsection II B, is based on the assumption that the interqubit coupling is turned on only between a pair of qubits which are in resonance. On the other hand, since the interaction between all pairs of qubits is always present, the real dynamics of the register of qubits, although coherent, is slightly different from the assumed. This deviation grows with time and limits the length of the coherent computation. In this appendix we estimate this effect in a register of $N \gg 1$ qubits treating the interaction term[§] $-\frac{1}{2} E_L \sum_{i < j} \rho_y^{(i)} \rho_y^{(j)}$ perturbatively.

Let us consider a time interval between two voltage switchings when the Hamiltonian is constant. During such an interval a single- or two-bit gate is performed, or it can be an idle period (which is normally not longer than an operation). We suppose that in the idle state the qubits are biased differently and their energy splittings are approximately equally separated by sufficiently large gaps, $\Delta E_\eta^{(i+1)} - \Delta E_\eta^{(i)} \approx \mathcal{E} \gg E_L$. During an operation the splittings for one or two bits are changed but this does not influence our estimate strongly.

As a first step, let us consider the effect of only one term in the sum in (15), $-\frac{1}{2} E_L \rho_y^{(i)} \rho_y^{(j)}$. We note that this term flips both qubits, and that the states $|0_i 0_j\rangle$ and $|1_i 1_j\rangle$ have very different energies, while the energy separation of $|0_i 1_j\rangle$ and $|1_i 0_j\rangle$ is small, \mathcal{E} , if $i = j \pm 1$. Therefore, the interaction term has a relatively small effect on the quantum evolution in the subspace $\{|0_i 0_j\rangle, |1_i 1_j\rangle\}$, while in the subspace $\{|0_i 1_j\rangle, |1_i 0_j\rangle\}$ the Hamiltonian is $\frac{1}{2} \begin{pmatrix} \mathcal{E} & -E_L \\ -E_L & -\mathcal{E} \end{pmatrix}$. Exponentiating, we obtain the evolution operator

[§]Since the $\tilde{\rho}$ -matrices can be obtained from the $\tilde{\sigma}$ -matrices by a y -rotation, the appearance of the interaction in terms of both sets of matrices is the same. The unperturbed Hamiltonian reads $\frac{1}{2} \sum_i \Delta E_\eta^{(i)} \rho_z^{(i)}$.

$$U(t) = \cos\left(\frac{\sqrt{\mathcal{E}^2 + E_L^2}}{2\hbar}t\right) - i \sin\left(\frac{\sqrt{\mathcal{E}^2 + E_L^2}}{2\hbar}t\right) \begin{pmatrix} \cos \epsilon & -\sin \epsilon \\ -\sin \epsilon & -\cos \epsilon \end{pmatrix}, \quad (\text{B1})$$

where $\tan \epsilon = E_L/\mathcal{E} \ll 1$, while in the absence of the perturbation one would have

$$U_0(t) = \cos\left(\frac{\mathcal{E}}{2\hbar}t\right) - i \sin\left(\frac{\mathcal{E}}{2\hbar}t\right) \begin{pmatrix} 1 & 0 \\ 0 & -1 \end{pmatrix}. \quad (\text{B2})$$

When applied to a state $|\ell\rangle$, (B1) and (B2) produce different results $U(\tau_{\text{op}})|\ell\rangle$ and $U_0(\tau_{\text{op}})|\ell\rangle$. We estimate the difference between both. Note that there are two contributions to $U - U_0$: due to different energies, $\sqrt{\mathcal{E}^2 + E_L^2}$ vs. \mathcal{E} , in the time-dependent arguments of trigonometric functions, and due to finite ϵ . The energy difference, however, is very small, contributing $\frac{E_L^2}{4\hbar\mathcal{E}}\tau_{\text{op}}$ to the deviation of U and U_0 , i.e. typically $\frac{E_L}{4\mathcal{E}}$ for 2-bit and $\frac{E_L^2}{4E_J\mathcal{E}}$ for single-bit gates. To estimate the other contribution, one can put $E_L = 0$ in the time-dependent sine- and cosine-functions in (B1). $U - U_0$ depends on the time span τ_{op} of the operation. If the operation is sufficiently long, $\tau_{\text{op}}\mathcal{E} \gg 1$ (this always holds for a 2-bit gate), the rms deviation is $\chi_2 = \frac{E_L}{\sqrt{2\mathcal{E}}}$. If a single-bit operation is performed and it is fast enough, $E_J \gg \mathcal{E}$, then the opposite inequality holds, $\tau_{\text{op}}\mathcal{E} \ll 1$, and the deviation is smaller, $\chi_1 = \frac{E_L}{2E_J}$. So in general, the rms deviation is $\chi = \chi_2$ during a 2-bit gate and $\chi = \min(\chi_1, \chi_2)$ during a single-bit gate.

Thus, we estimated the effect of one term in the sum (15). Now we take all the terms into account. To find $U - U_0$ in this case, we estimate their effects on an initial (at the beginning of the period between voltage switchings) multi-qubit logical state $|\ell\rangle$ of the kind $|00101\dots\rangle$. The interaction term produces a correction to $|\ell\rangle$ which is a superposition of other logical states with close energies. As follows from the analysis above, this superposition is dominated by the states which differ from $|\ell\rangle$ by the flip of adjacent zero and unity. The number of such “neighbours” of the state $|\ell\rangle$ is at most $N - 1$, the number of pairs of adjacent bits. Averaging over different states $|\ell\rangle$ we get the typical number $(N - 1)/2$ of “neighbours”. Therefore, the typical rms deviation during a gate is $\chi\sqrt{(N - 1)/2}$. If deviations during consecutive gates are uncorrelated, the process is diffusive and after $\sim 2/(N\chi^2)$ gates the deviation grows to essential values of order one and further computation makes no sense.

To estimate the maximal possible value of \mathcal{E} we note that the maximal splitting, $N\mathcal{E}$, is limited from above by $\hbar\omega_{LC}^{(N)}$ (9). In order not to excite different charge states with integer $n \neq 0, 1$ as well as the state $n = 1/2$ (an unpaired electron), $N\mathcal{E}$ should additionally not exceed $2E_{\text{qb}}$ and $\Delta - E_{\text{qb}}$, respectively. With our choice of parameters however, $\hbar\omega_{LC}^{(N)}$ is a stronger limitation.

Using this value of $\mathcal{E} = \hbar\omega_{LC}^{(N)}/N$ we conclude that the number of 2-bit gates is limited by $4N^{-4}(\hbar\omega_{LC}^{(N=1)}/E_L)^2$ and the number of single-bit operations by the larger of this number and $8N^{-1}(E_J/E_L)^2$.

¹ K.K. Likharev. Proc. IEEE, to be published (1999).
² S. Lloyd, Science **261**, 1589 (1993); C.H. Bennett, Physics Today **48** (10), 24 (1995); A. Barenco, Contemp. Phys. **37**, 375 (1996); D.P. DiVincenzo, Science **269**, 255 (1995), and in *Mesoscopic Electron Transport*, ed. L.L. Sohn et al., Kluwer, 1997.
³ J.I. Cirac and P. Zoller, Phys. Rev. Lett. **74**, 4091 (1995).
⁴ B.E. King et al., Phys. Rev. Lett. **81**, 1525 (1998).
⁵ B.E. Kane, Nature **393**, 133 (1998); D. Loss and D.P. DiVincenzo, Phys. Rev. A **57**, 120 (1998); G. Burkard et al., cond-mat/9808026.
⁶ R. Rouse, S. Han, and J.E. Lukens, Phys. Rev. Lett. **75**, 1614 (1995).
⁷ J.E. Mooij, private communication; cf. also L.B. Ioffe et al., preprint, cond-mat/9809116.
⁸ C. Cosmelli et al., to be published in ‘Quantum Coherence and Decoherence – ISQM – Tokyo 98’, North-Holland Publ. Delta Series.
⁹ A. Shnirman, G. Schön, and Z. Hermon, Phys. Rev. Lett. **79**, 2371 (1997).
¹⁰ D.V. Averin, Solid State Commun. **105**, 659 (1998).
¹¹ V. Bouchiat, Ph. D. Thesis, Université Paris 6 (1997); V. Bouchiat, D. Vion, P. Joyez, D. Esteve, and M.H. Devoret, Physica Scripta **T76**, 165 (1998).
¹² A. Maassen van den Brink, G. Schön, and L.J. Geerligs, Phys. Rev. Lett. **67**, 3030 (1991).
¹³ M.T. Tuominen, J.M. Hergenrother, T.S. Tighe, and M. Tinkham, Phys. Rev. Lett. **69**, 1997 (1992).
¹⁴ J. Siewert and G. Schön, Phys. Rev. B **54**, 7421 (1996).
¹⁵ Y. Nakamura, C.D. Chen, and J.S. Tsai, Phys. Rev. Lett. **79**, 2328 (1997).
¹⁶ P. Hadley, E. Delvigne, E.H. Visscher, S. Lähteenmäki, and J.E. Mooij, preprint.
¹⁷ Yu. Makhlin, G. Schön, and A. Shnirman, preprint, cond-mat/9808067.
¹⁸ A. Shnirman and G. Schön, Phys. Rev. B **57**, 15400 (1998).
¹⁹ Y. Levinson, Europhys. Lett. **39**, 299 (1997).
²⁰ I.L. Aleiner et al., Phys. Rev. Lett. **79**, 3740 (1997).
²¹ S.A. Gurvitz, Phys. Rev. B **56**, 15215 (1997).
²² E. Buks, R. Schuster, M. Heiblum, D. Mahalu, and V. Umansky, Nature, **391**, 871 (1998).
²³ P. Lafarge et al., Phys. Rev. Lett. **70**, 994 (1993).
²⁴ G. Schön and A.D. Zaikin, Europhys. Lett. **26**, 695 (1994).
²⁵ M. Tinkham, *Introduction to Superconductivity*, 2nd edition, McGraw-Hill (1996).
²⁶ A.O. Caldeira and A.J. Leggett, Ann. Phys. (NY) **149**, 374 (1983).
²⁷ S.V. Panyukov and A.D. Zaikin, J. Low. Temp. Phys. **73**, 1 (1988).

²⁸ A.A. Odintsov, Sov. Phys. JETP **67**, 1265 (1988).

²⁹ Yu.V. Nazarov, Sov. Phys. JETP **68**, 561 (1989).

³⁰ M.H. Devoret, D. Esteve, H. Grabert, G.L. Ingold, and H. Pothier, Phys. Rev. Lett. **64**, 1824 (1990).

³¹ A.J. Leggett, S. Chakravarty, A.T. Dorsey, M.P.A. Fisher, A. Garg and W. Zwerger, Rev. Mod. Phys. **59**, 1 (1987).

³² U. Weiss and M. Wollensak, Phys. Rev. Lett. **62**, 1663 (1989); R. Görlich, M. Sassetti and U. Weiss, Europhys. Lett. **10**, 507 (1989).

³³ L.P. Kouwenhoven, private communication.

³⁴ P.W. Shor, Phys. Rev. A, **52**, 2493 (1995); A. Steane, Proc. Roy. Soc. of London A, **452**, 2551 (1996); E.H. Knill and R. Laflamme Phys. Rev. A **55**, 900, (1997); E. Knill, R. Laflamme and W. Zurek, Science, **279**, 342 (1998).

³⁵ V. Ambegaokar, U. Eckern and G. Schön, Phys. Rev. Lett. **48**, 1745 (1982); G. Schön and A.D. Zaikin, Physics Reports **198**, 237 (1990).

³⁶ H. Schoeller and G. Schön, Phys. Rev. B **50**, 18436 (1994).

³⁷ Yu.V. Nazarov, Physica B **189**, 57 (1993); T.H. Stoof and Yu.V. Nazarov, Phys. Rev. B **55**, 1050 (1996); S.A. Gurvitz and Ya.S. Prager, Phys. Rev. B **53**, 15932 (1996).

³⁸ D.V. Averin and K.K. Likharev, in *Mesoscopic Phenomena in Solids*, edited by B.L. Altshuler, P.A. Lee, and R.A. Webb (Elsevier, Amsterdam, 1991), p. 173.

³⁹ A. Stern, Y. Aharonov, and Y. Imry, Phys. Rev. A **41**, 3436 (1990).

⁴⁰ A.N. Korotkov, preprint, quant-ph/9807051.

⁴¹ S.A. Gurvitz, preprint, quant-ph/9808058.

⁴² L. Stodolsky, preprint, quant-ph/9805081.

⁴³ D.J. Wineland, C. Monroe, W.M. Itano, D. Leibfried, B. King, and D.M. Meekhof, J. Res. Natl. Inst. Stand. Tech. **103**, 259 (1998).